United States
Department of
Agriculture

Forest Service

Forest Health
Protection

Forest Health
Technology
Enterprise Team-
Davis
2121C Second Street
Davis, CA 95616

DUGWAY TOWER FLYBY DATA COLLECTION, REDUCTION AND INTERPRETATION

FHTET 96-37
December 1996

Pesticides used improperly can be injurious to human beings, animals, and plants. Follow the directions and heed all precautions on labels. Store pesticides in original containers under lock and key—out of the reach of children and animals—and away from food and feed.

Apply pesticides so that they do not endanger humans, livestock, crops, beneficial insects, fish, and wildlife. Do not apply pesticides where there is danger of drift when honey bees or other pollinating insects are visiting plants, or in ways that may contaminate water or leave illegal residues.

Avoid prolonged inhalation of pesticide sprays or dusts; wear protective clothing and equipment, if specified on the label.

If your hands become contaminated with a pesticide, do not eat or drink until you have washed. In case a pesticide is swallowed or gets in the eyes, follow the first aid treatment given on the label, and get prompt medical attention. If a pesticide is spilled on your skin or clothing, remove clothing immediately and wash skin thoroughly.

NOTE: Some States have restrictions on the use of certain pesticides. Check your State and local regulations. Also, because registrations of pesticides are under constant review by the U.S Environmental Protection Agency, consult your local forest pathologist, county agriculture agent, or State extension specialist to be sure the intended use is still registered.

FHTET 96-37
(C.D.I. Technical Note 88-11)
December 1996

Dugway Tower Flyby Data Collection, Reduction and Interpretation

Prepared by:

Milton E. Teske
Andrew E. Kaufman
Thomas B. Curbishley

Continuum Dynamics, Inc.
P.O. Box 3073
Princeton, NJ 08543

P.O. No. D8-444
(October 1988)

Prepared for:

Lockheed - EMSCO
P.O. Box 217, Bldg. 6002
Dugway, UT 84022

USDA Forest Service
Forest Health Technology
Enterprise Team
2121C Second Street
Davis, CA 95616
(916) 757-8341

EXECUTIVE SUMMARY

On October 3 and 4 sixteen passes were made by an F-4 high speed fighter aircraft normal to a row of ten towers holding propeller anemometers. These anemometers measured the wind speed generated by the aircraft wake at 32 locations. The vortex circulation time history was then inferred by a generalized vortex-locating algorithm developed for previous comparisons with slower speed aircraft data from Program WIND. These data results were then fit by least squares to the AGDISP/FSCBG circulation decay model. Representative atmospheric turbulence levels were recovered for these runs, and the decay coefficient was determined.

These results extend the applicability of the Program WIND results to the higher aircraft speed regime. The quantity defined by decay coefficient times turbulence level is shown to be within the standard deviation of the previous Program WIND results, and suggests that a mean value of 0.56 m/sec is an acceptable input parameter across all aircraft speed regimes. For the turbulence levels determined at the Dugway test site, the decay coefficient is seen to vary between near-zero to a value of 2.5 . This result correlates well with a theoretical atmospheric decay coefficient of 0.41 .

TABLE OF CONTENTS

1. INTRODUCTION

Program WIND ("Winds in Nonuniform Domains") was performed in phases jointly by the United States Department of Agriculture Forest Service and the United States Army at several sites in northern California. Phase I was conducted from May through July, 1985 at a cleared and forested site (Foresthill Seed Orchard) and an almond orchard (Hennigan Almond Orchard north of Chico); and Phase III, from late April to early May, 1986 at a cleared sloping site in the Sierra Nevada foothills near Red Bluff. In both of these experimental studies, anemometer tower grids recorded the ambient vertical velocity time histories as various slow speed aircraft repeatedly traversed normal to the grid. These digitized velocity traces produced an aircraft wake signature that could be used to infer the strength and lateral and vertical motion of the aircraft vortex pairs generating the traces. A previous report (Ref. 1) summarizes the examination of this data base by using a generalized algorithm to locate the trailed vortex pairs in all available data, and to infer their decay properties in the atmosphere. This decay effect was then quantified as a decay coefficient range for subsequent input in the AGDISP and FSCBG codes (Refs. 2 and 3).

In the Phase I tests the tower grid included anemometers for both horizontal and vertical velocities, with a total of 32 anemometers available for the analog-to-digital system employed to record the data. This study determined that the horizontal velocity signals would be easily polluted by any crosswind velocity component, giving a decidedly incorrect impression of the vortex position and strength. Also, the closeness of the tower grid (the towers were spaced 2.7 to 6.1 meters apart with seven towers) meant that no more than 20 to 40 seconds of data could be taken before the vortices would drift off the grid. Thus, in the Phase III tests the towers contained only vertical velocity anemometers, and were spaced uniformly apart at 6.1 meters (with ten towers). A longer sampling time was used to track the vortices across this wider tower grid.

On October 3 and 4 a series of flights at Dugway, Utah, were made by a high speed fighter aircraft over a tower grid similar to the Phase III tests. The higher anticipated speeds of the aircraft suggested that the vortex pair created as the aircraft wake would be weak and therefore more difficult to detect. Consequently, the towers were extended to 15.2 meters in altitude and spaced 12.2 meters apart (again ten towers) in an attempt to capture the passage of the vortex pair. The sampling time was continued until the anemometers appeared visually to cease rotating.

The test procedure followed at Dugway is summarized in Section 2 of this report. Section 3 reviews the generalized algorithm used to reduce the data, and Section 4 compares the vortex circulation decay data with previous results. Conclusions are offered in Section 5.

2. SUMMARY OF TESTS CONDUCTED

The test procedure on-site at Dugway, Utah, is reviewed in this section of the report.

2.1 Test Aircraft

The aircraft used in all passes over the tower grid was an F-4 high speed fighter aircraft. The intent of the test series was to extend the aircraft flight speed well beyond the aircraft speeds in Program WIND. In order to have a good chance of capturing the vortex pair in the tower grid, however, the aircraft would have to be flown as close to the top of the towers as feasible.

2.2 Test Site

All tests were performed over the flat terrain near Dugway, Utah, with the tower grid set perpendicular to an access road (Tango Road) to offer a visual cue to the pilot. Initially, smoke pots were also used to identify the road. Ten towers were spaced uniformly apart and instrumented with propeller anemometers as shown in Figure 2-1. Data acquisition was housed in a command trailer centered on the anemometer grid approximately 10 meters east of the tower line. The site was suggested because it was anticipated that local horizontal winds would be less than 1 m/sec nominally.

The towers used to mount the anemometers were telescoping masts extended to their maximum height of 15.2 m. The towers were placed in a single line normal to the road at 12.2 m intervals, yielding a grid span of 110.0 m . The anemometers were mounted vertically at 3.3 , 8.6 and 14.1 m from the ground on each tower. In addition to the vertical sensors, U-V-W sensors were mounted on tower 0 at 15.1 m and on tower 9 at 8.6 m .

2.3 Anemometers

Gill anemometers manufactured by the R.M. Young Company, on loan to the U.S. Forest Service from the Transportation Systems Center of the U.S. Department of Transportation were used for this study. Four-bladed propellers (19 cm in diameter) were coupled with the DC generators to complete the anemometer and were calibrated at 1800 rpm. The anemometers were mounted on the towers oriented vertically to measure the vertical velocities of the wake. The anemometers were electrically connected to the data acquisition system with filtering capacitors in accordance with manufacturer's recommendations. The wake velocity signals were sampled and

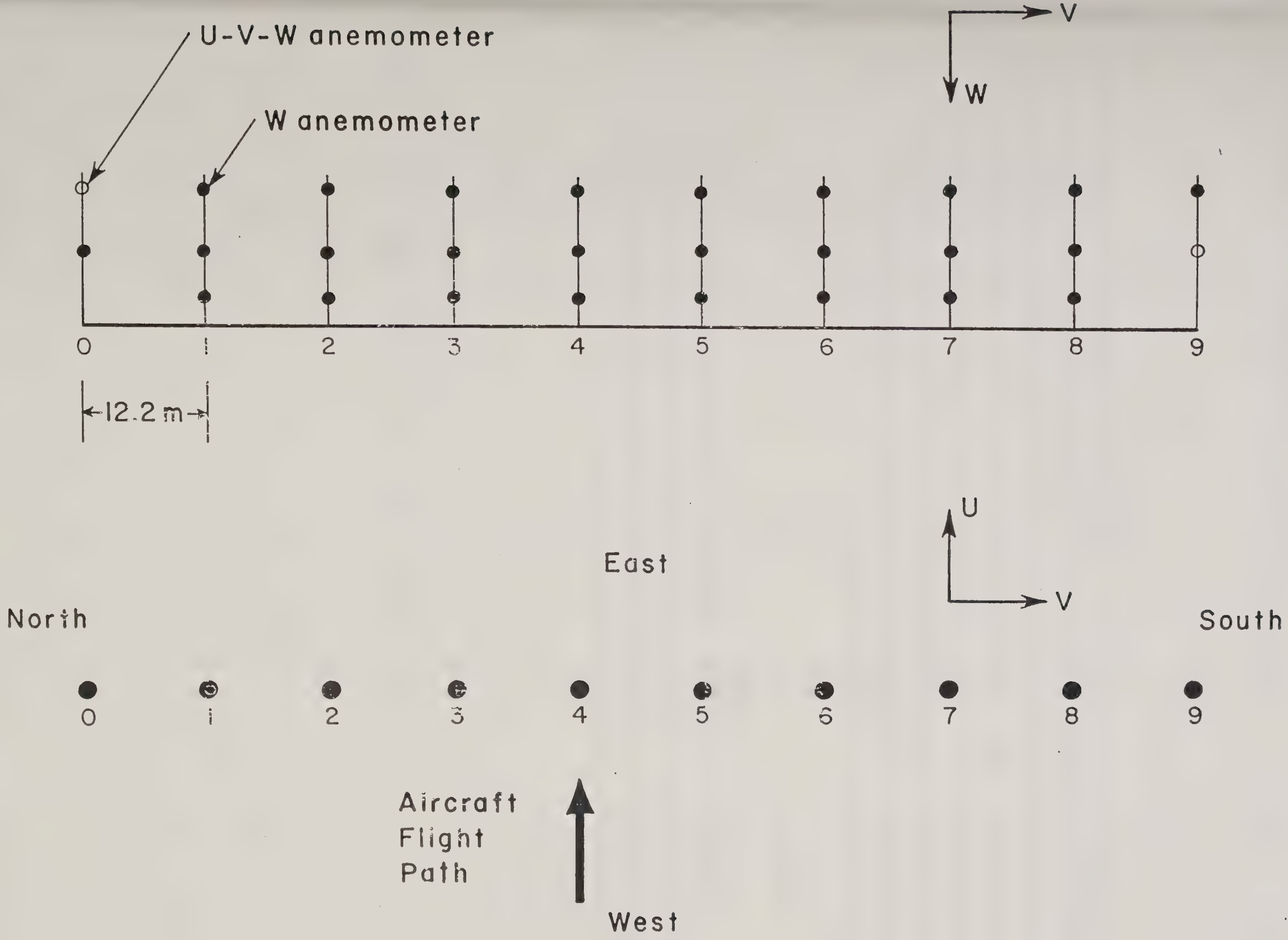

Figure 2-1: The Dugway anemometer tower grid configuration.

recorded by a digital data acquisition system during the aircraft flight over the towers. U-V-W sampling was also done prior to each aircraft run.

2.4 Data Acquisition System

The data acquisition system consisted of an IBM Portable PC with two Data Translation DT2801 auxiliary boards to sample and digitize 32 channels of analog voltage signals from the anemometers. Sampling was carried out at a rate of 100 samples/sec (each anemometer was sampled every 0.34 sec). The full scale analog voltages ±1.25 volts were converted to the digital representations 0 to 4095 , and stored in memory. A maximum of four minutes of data could be sampled continuously (before reaching memory limits) and stored for post-test conversion to engineering units and further analysis. Sampling began before the aircraft flyover, to provide U-V-W data to extract the mean wind conditions.

2.5 Test Matrix

The objective to the test program was to collect high speed aircraft wake data (vortex trajectories) to compare with the slower speed results found from the Program WIND tests. The complete matrix is given in Table 2-1. No data was collected for run 3 because data reduction was not complete before the aircraft returned for the next pass.

TABLE 2-1. DUGWAY TEST MATRIX

RUN	DAY	TOWER	HEIGHT (Meters)	SPEED (Knots)	REMARKS
1	10/03	Center	45.7	525	Note 1
2	10/03	Center	45.7	525	Note 1
3	10/03				No Data
4	10/03	Center	30.5	400	Note 1
5	10/03	Center	30.5	425	Note 1
6	10/03	Center	30.5	350	Note 1
7	10/03	Center	30.5	350	
8	10/03	2 - 3	30.5	300	
9	10/03	3	30.5	300	
10	10/03	3 - 4	30.5	300	Note 2
11	10/03	1	30.5	300	Note 2
12	10/03	1	30.5	300	Note 2
13	10/03	1	30.5	300	Note 2
14	10/04	7	30.5	315	Full Tanks
15	10/04	8	30.5	300	No Tanks
16	10/04	7	30.5	300	Full Tanks

Note 1: Anemometers on the top row on towers 5 and 6 were inoperative.

Note 2: Anemometers on the top row on tower 5 experienced a broken blade.

3. GENERALIZED ALGORITHM FOR DETERMINING VORTEX TRAJECTORIES

Reference 1 summarizes the generalized algorithm for inferring the location and strength of the vortex pair traveling through an anemometer tower grid. That analysis is reviewed here.

An aircraft wake may be represented by a simple vortex pair (with its image pair below the surface, Figure 3-1), each vortex of which may be characterized by a velocity field of the form

$$v = \frac{\Gamma}{2\pi} \frac{R}{\left(R_c^2 + R^2\right)} \tag{3-1}$$

where

v = velocity magnitude
Γ = vortex circulation strength
R = radius from vortex center
R_c = vortex core radius, a constant

The resultant velocity at any point in the flow field (in particular, at an anemometer location) is then the algebraic sum of the velocity contributions from the four vortices acting on the flow. The aircraft vortex pair is located in a coordinate system relative to the tower grid (Figure 3-2). The wake model introduces four unknowns that must be deduced from the data in any run at any time at which data are collected. These unknowns are the vortex circulation strength and the three spatial dimensions

h = the height of the vortex pair above the surface
s = the semispan of the vortex pair (the half distance between their centers)
d = the offset distance of the aircraft centerline from the leftmost anemometer tower

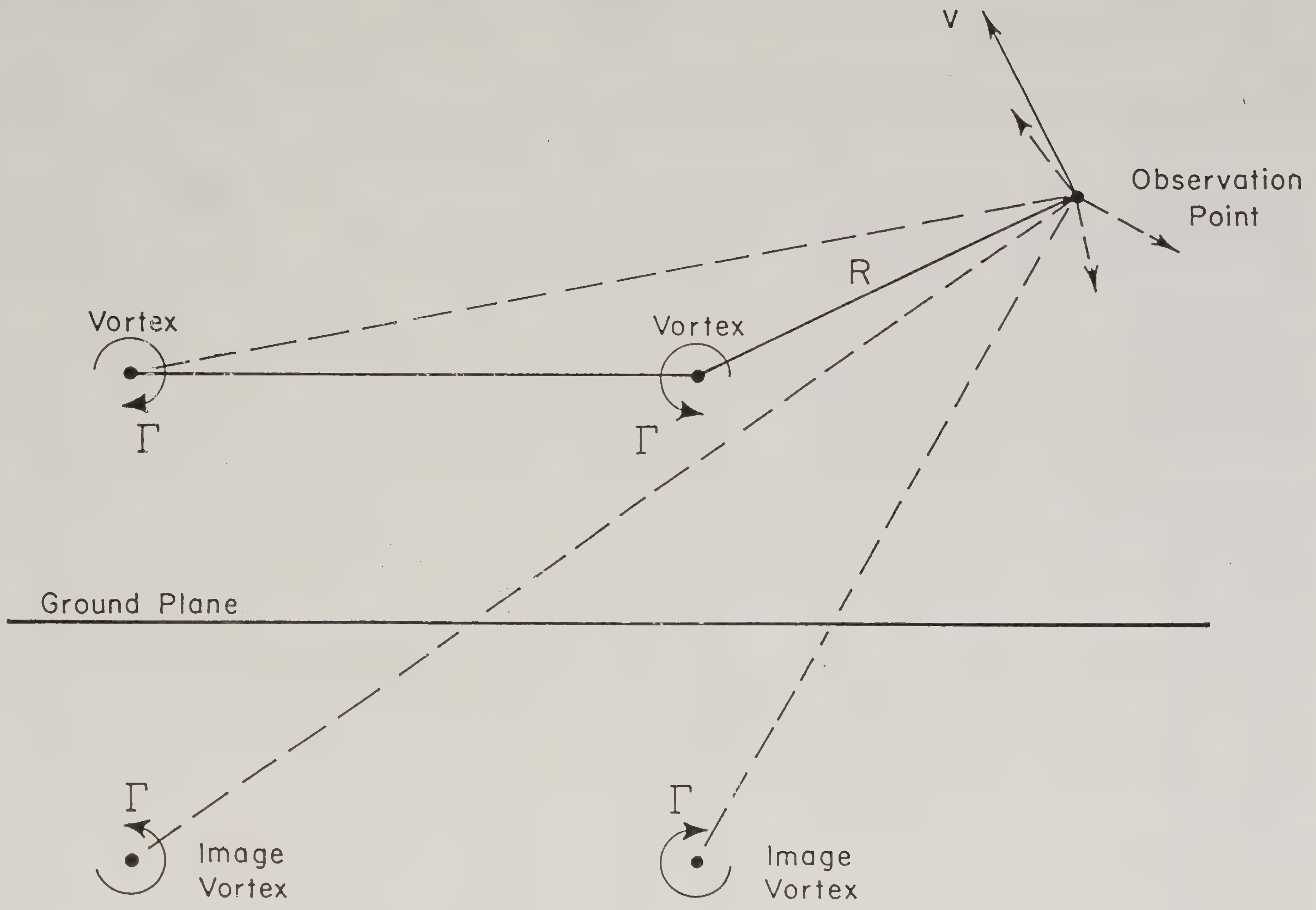

Figure 3-1: The composite velocity vector at an observation point found by summing the contributions of the aircraft vortex pair and its image system below the ground plane.

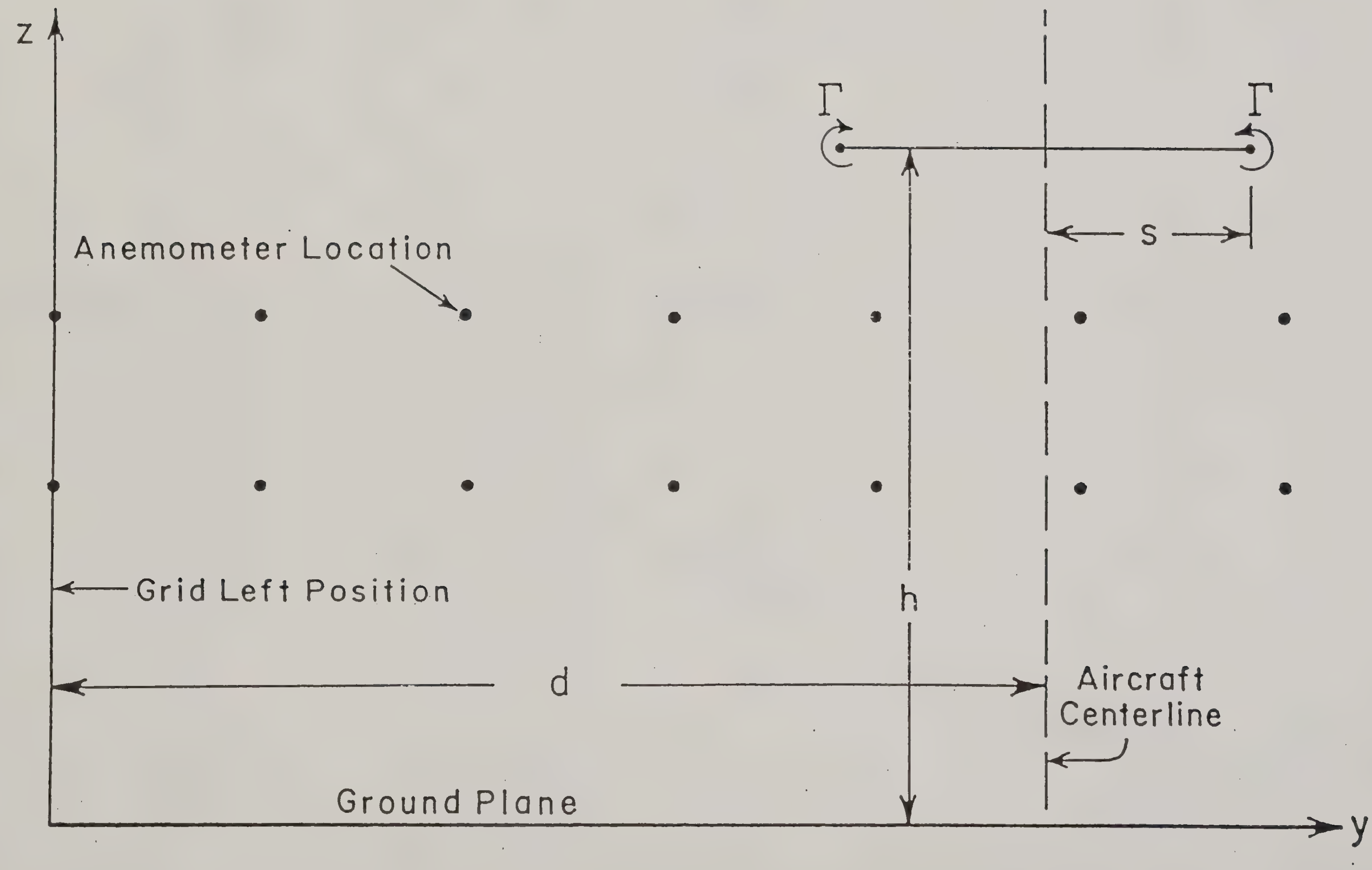

Figure 3-2: The aircraft vortex pair located relative to the anemometer tower grid. The relevant lengths are the height of the vortex pair h, the semispan distance between the vortices s, and the offset d of the aircraft centerline from the grid left position.

Aircraft wake physics are only approximated by the simple velocity law given in Eq. (3-1). Thus, the intent of the generalized analysis is to seek a solution for these four parameters in any run at any time so as to minimize the error in the velocity predictions at all of the anemometer locations. With four unknowns and many more anemometer locations, the problem may be cast into a least squares analysis by defining an error E as

$$E = \sum_{n=1}^{N} \left(w_n - \overline{w}_n\right)^2 \tag{3-2}$$

where the overbar denotes the data, and the index n is from 1 to N, the total number of anemometers. The error E is a positive definite quantity. The vertical velocities w are determined by summing the contributions of the four vortices in the model, calculated for specific values of the parameters Γ, h, s and d. The data $\overline{w}$ are found directly from the test results.

A crucial physical observation is made at this point: if the experimental data were normalized by any positive value, the resulting velocity vectors could still be used to infer the spatial position of the vortex pair in the anemometer field irrespective of the actual vortex circulation strength. This observation implies that locating the vortex pair involves the solution for h, s and d without regard to the value of Γ.

The approach used here normalizes the vertical velocities in the error equation by their respective root mean square velocities to give

$$E^* = \sum \left[\left(\frac{w_n}{w_{rms}}\right) - \left(\frac{\overline{w}_n}{\overline{w}_{rms}}\right) \right]^2 \tag{3-3}$$

where

$$w_{rms} = \sqrt{\frac{1}{N} \sum w_n^2} \tag{3-4}$$

$$\overline{w}_{rms} = \sqrt{\frac{1}{N} \sum \overline{w}_n^2}$$

Because the predicted vertical velocities are all linear in vortex circulation strength Γ, this modification to the error removes Γ from the equation for E^* and recasts the problem into one involving the three parameters h, s and d.

Equation (3-3) for E^* is nonlinear in h, s and d, but may be analytically differentiated with respect to these unknowns to give

$$F_h = \partial E^*/\partial h$$

$$F_s = \partial E^*/\partial s \tag{3-5}$$

$$F_d = \partial E^*/\partial d$$

Clearly, when all three derivatives in Eq. (3-5) tend to zero, the slope of E^* also tends to zero and E^* reaches a local minimum. These F functions are nonlinearly related to h, s and d. At any value set of (h,s,d), the local values of the F's in Eq. (3-5) may be determined analytically to generate partial derivatives of the form $\partial F/\partial h$, $\partial F/\partial s$, $\partial F/\partial d$ to construct the model equation for F (representing F_h, F_s and F_d) of the form

$$\Delta F = \frac{\partial F}{\partial h} \Delta h + \frac{\partial F}{\partial s} \Delta s + \frac{\partial F}{\partial d} \Delta d \tag{3-6}$$

The partial derivatives in this equation are known as influence coefficients. For any value of (h,s,d), the values of the three partial derivatives and F may be generated. Since the solution requires F to tend to zero, the left-hand side of Eq. (3-6) may be specified by

$$\Delta F = -F \tag{3-7}$$

The complete system may be seen to be a three-equation system for the values $(\Delta h,\Delta s,\Delta d)$ to add to the present values (h,s,d) to give new values $(h+\Delta h,s+\Delta s,d+\Delta d)$ to recompute E^*

and drive the solution to a minimum. This iteration procedure is followed at every time in the test run being analyzed.

Once values for (h,s,d) have been determined, the original error E may be differentiated to give

$$F_{\Gamma} = \partial E/\partial \Gamma = 0 \tag{3-8}$$

to find the minimum of E and determine Γ . This equation is solved easily because the equation for F is linear in Γ . With the solution in hand for (Γ,h,s,d) , these values are used as initial guesses for the next time in the run being analyzed. All results have been computed with a core size of $R_c = 0.15$ meters.

Figures 3-3 to 3-17 present the results of applying the generalized algorithm to all applicable data. In all cases the time of 0 seconds is the time of initiation of the data acquisition system. The algorithm was started after 5 seconds of data collection in an attempt to begin data reduction when a vortex pair could be expected in or near the tower grid. The horizontal or Y distance is measured from the leftmost tower 0 . The vortex pair track horizontally and vertically is shown in these figures along with the inferred circulation strength. The dashed curve in the circulation plot is a best fit to the vortex decay model. It may be seen that most of the runs provide excellent correlation with the circulation decay model of Eq. (4-1) below.

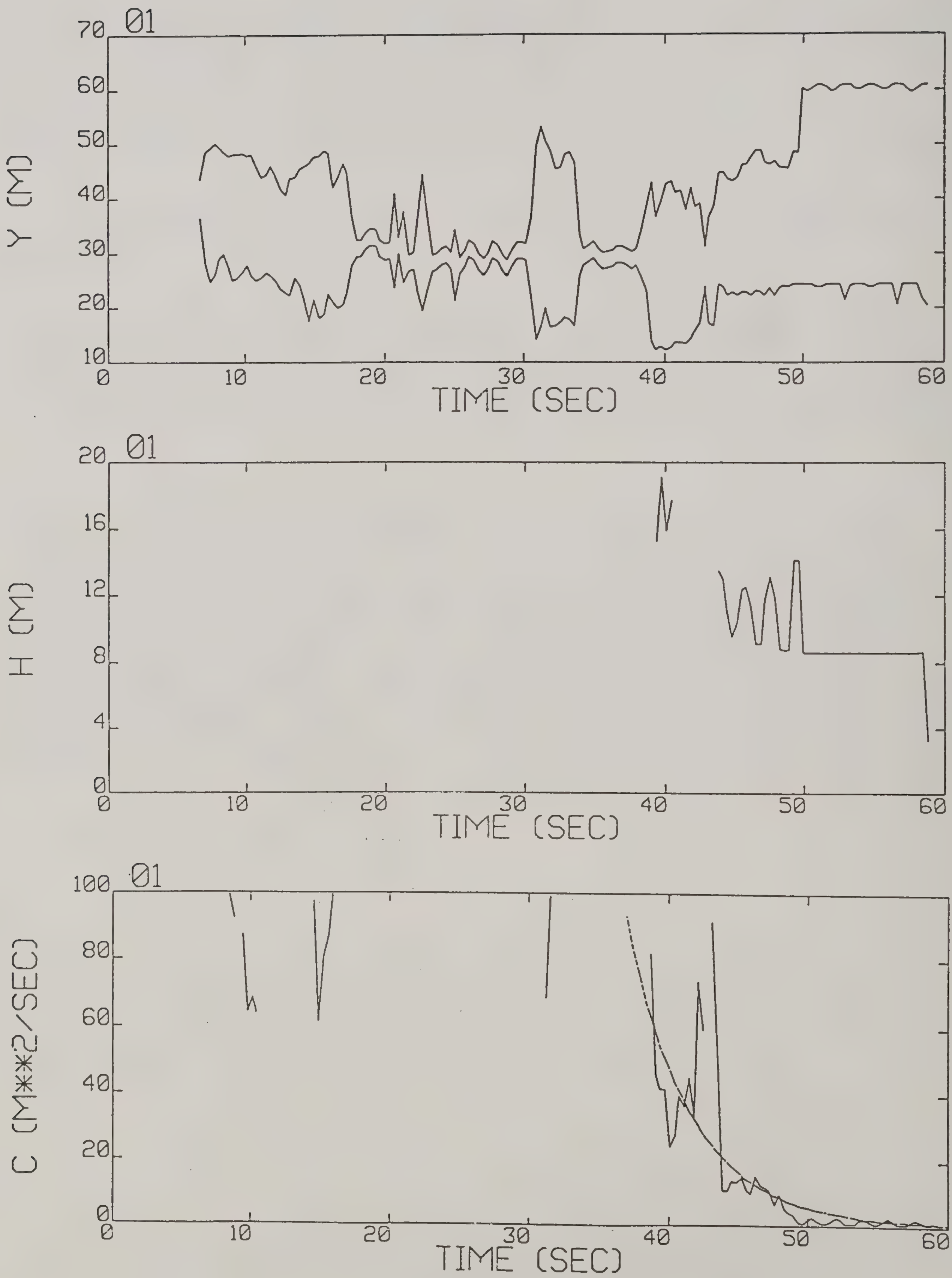

Figure 3-3: Generalized algorithm track through the anemometer data for run 1 at Dugway: lateral position of the left and right vortices (top); height (middle); circulation (bottom); circulation decay curve (dashed).

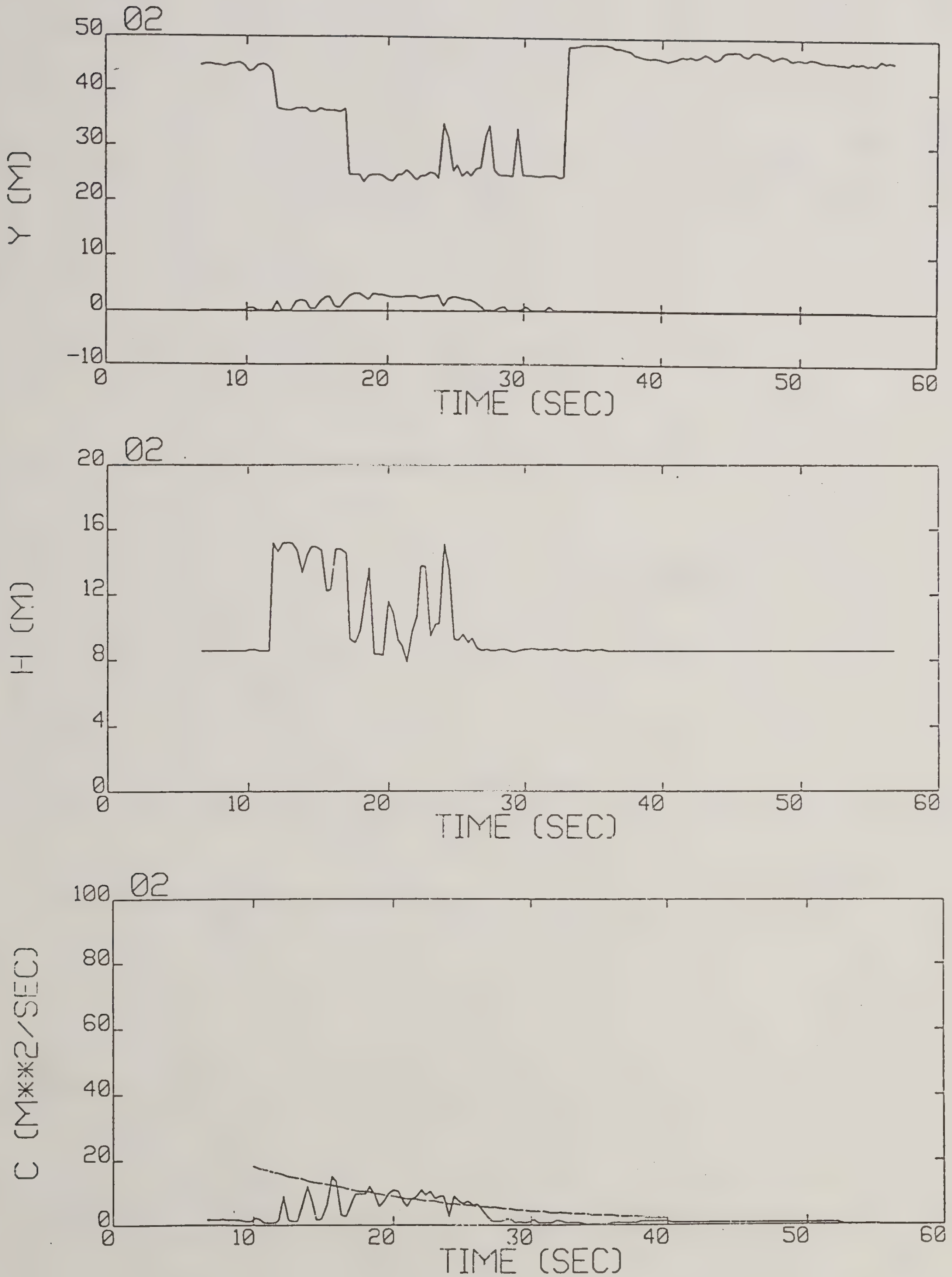

Figure 3-4: Track for run 2 at Dugway.

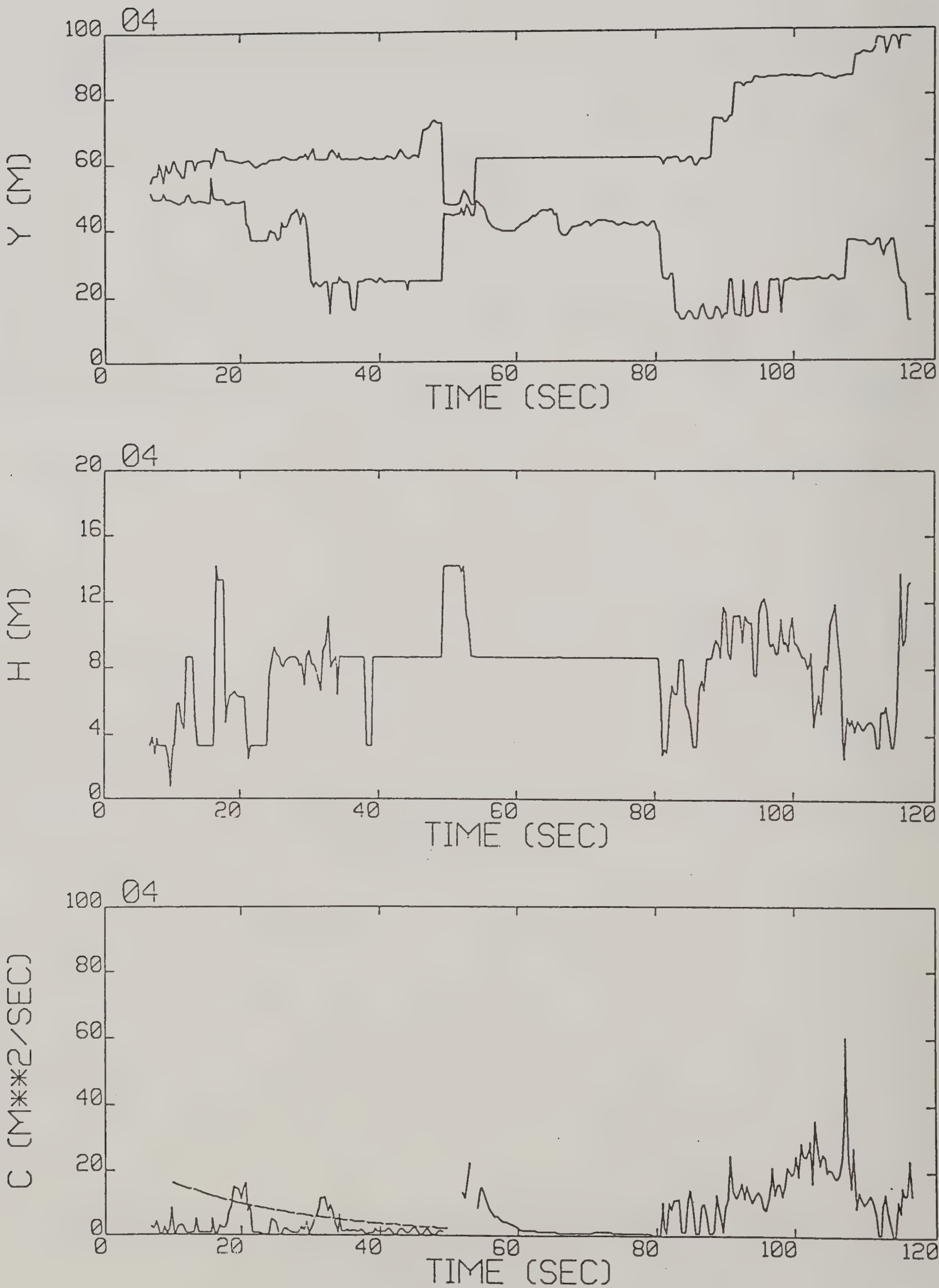

Figure 3-5: Track for run 4 at Dugway.

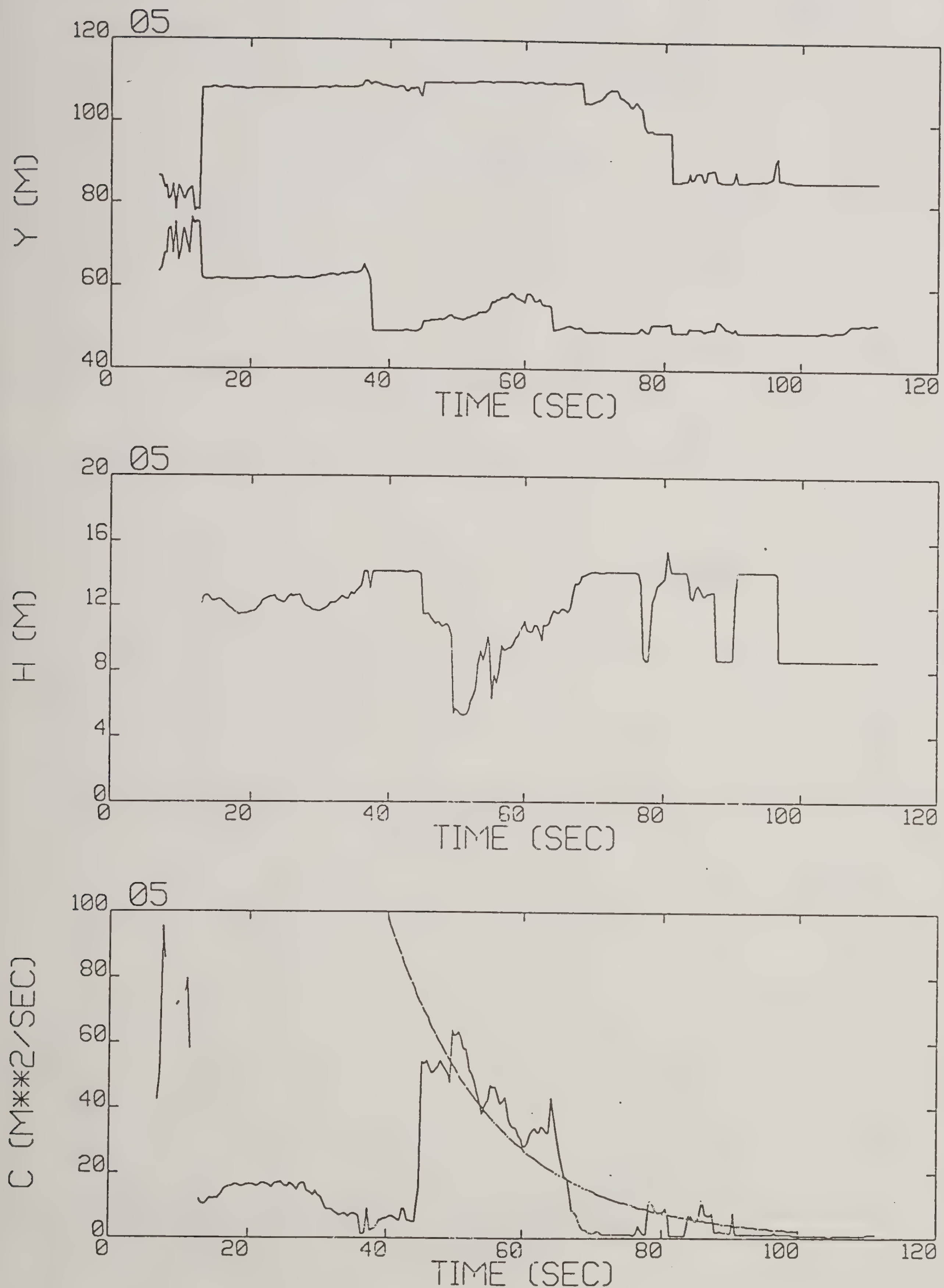

Figure 3-6: Track for run 5 at Dugway.

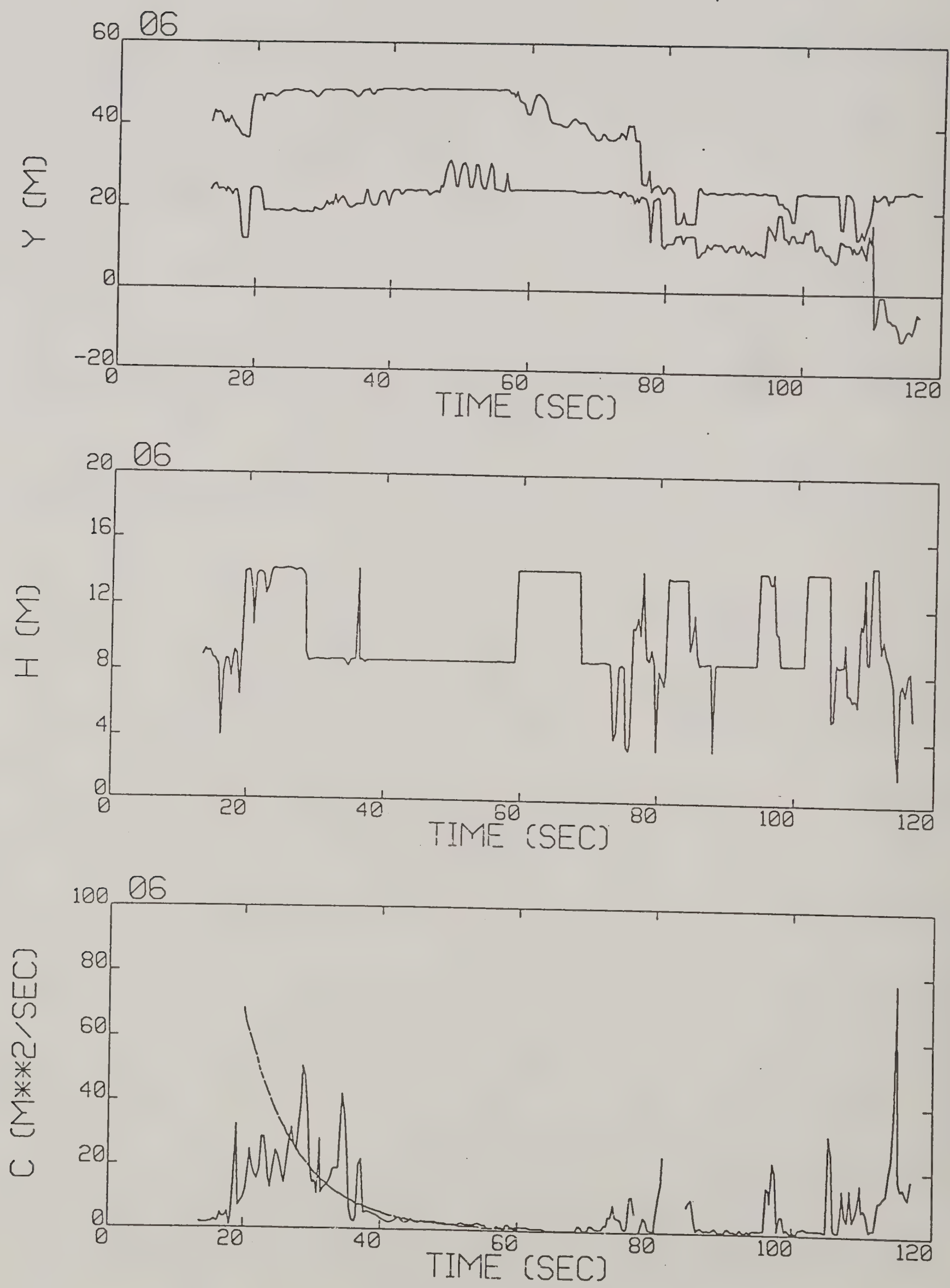

Figure 3-7: Track for run 6 at Dugway.

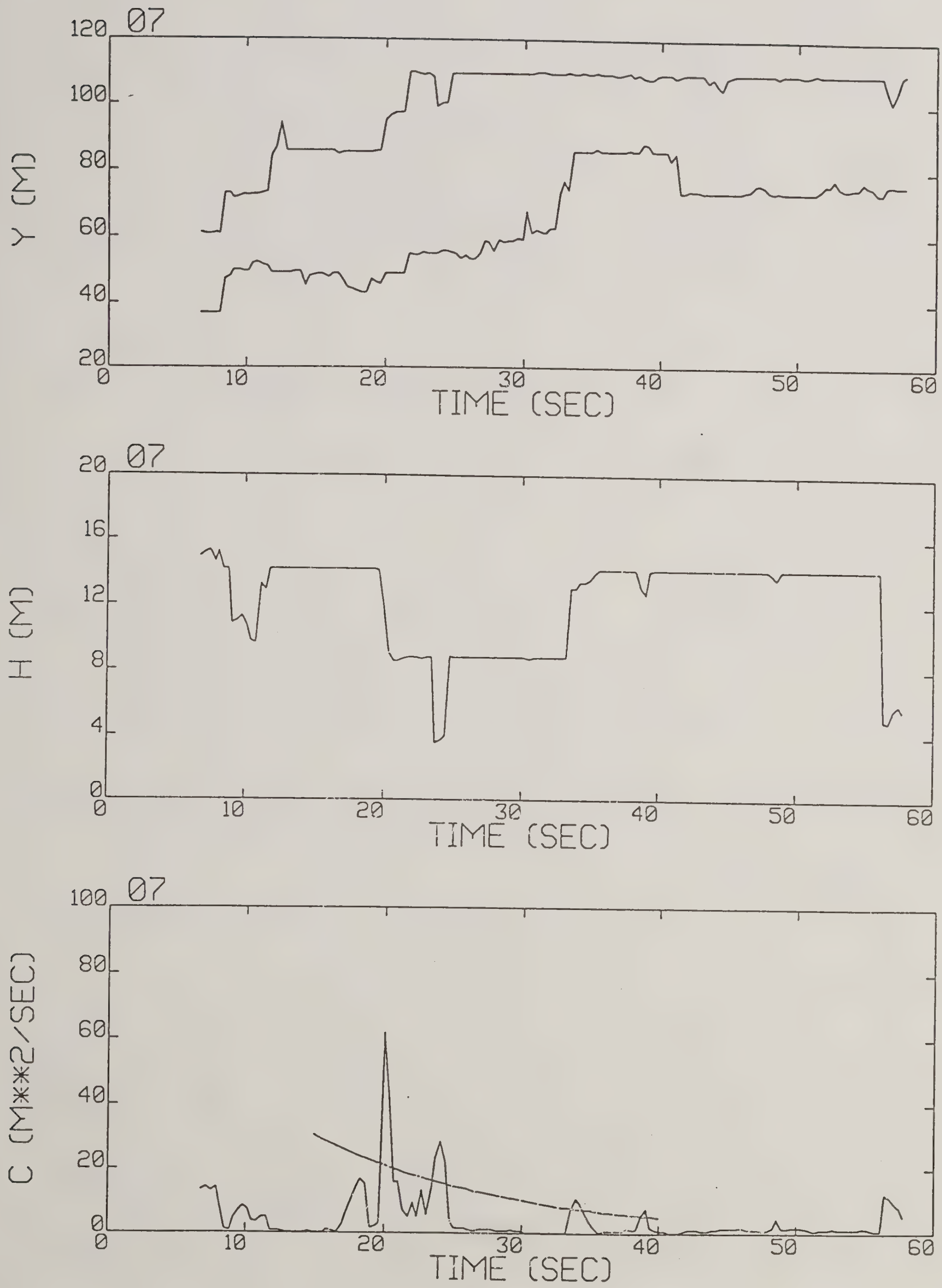

Figure 3-8: Track for run 7 at Dugway.

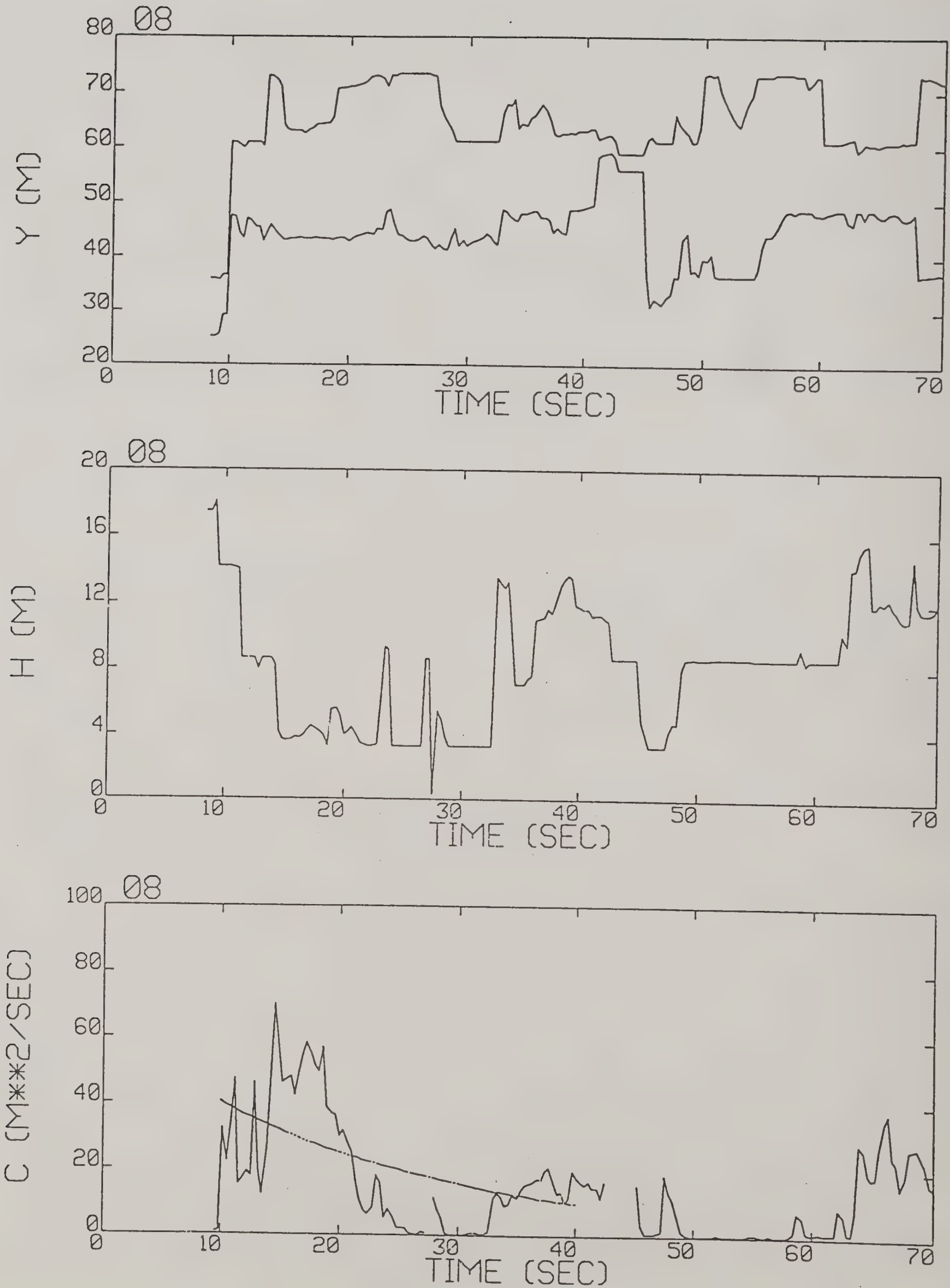

Figure 3-9: Track for run 8 at Dugway.

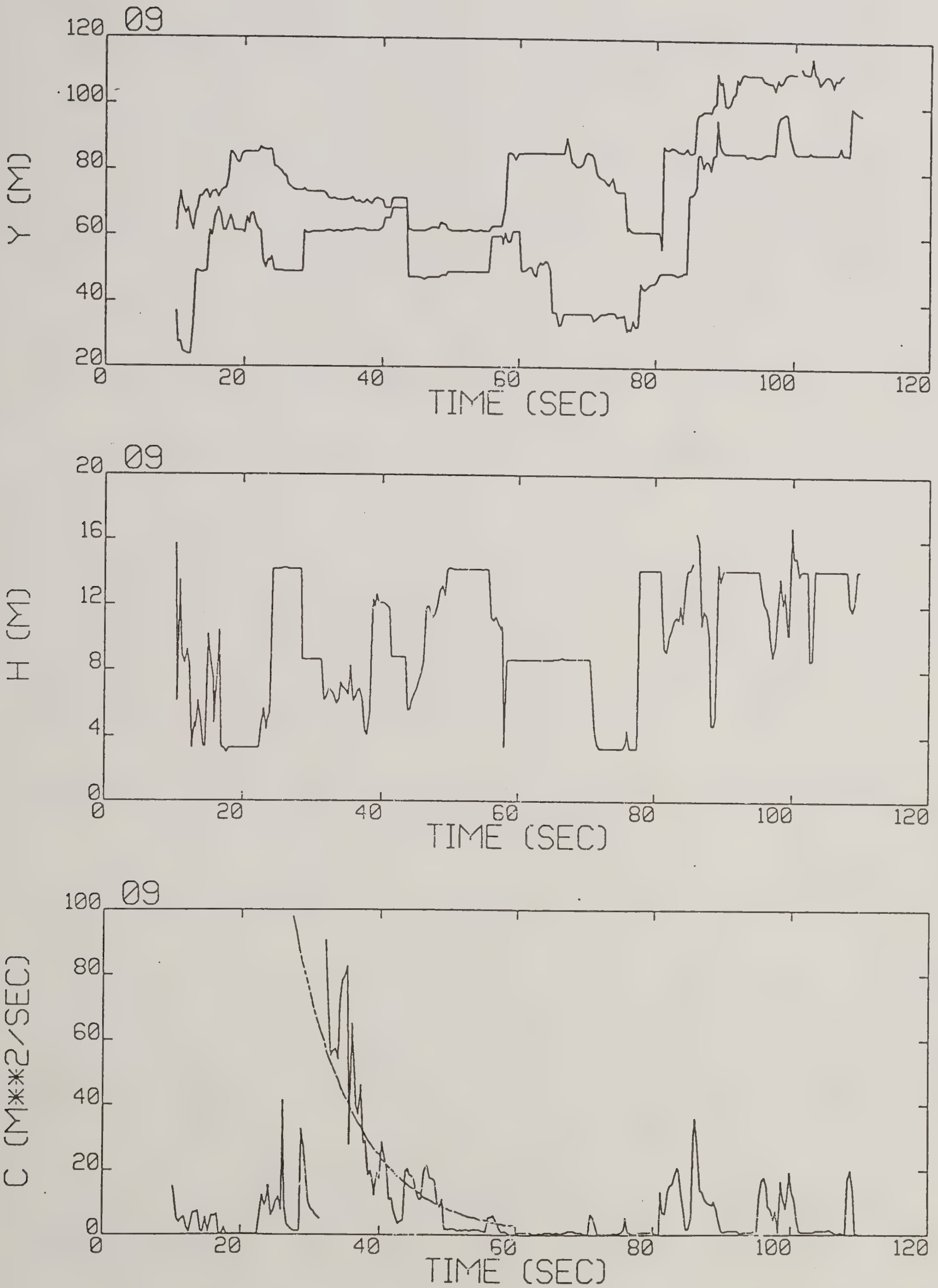

Figure 3-10: Track for run 9 at Dugway.

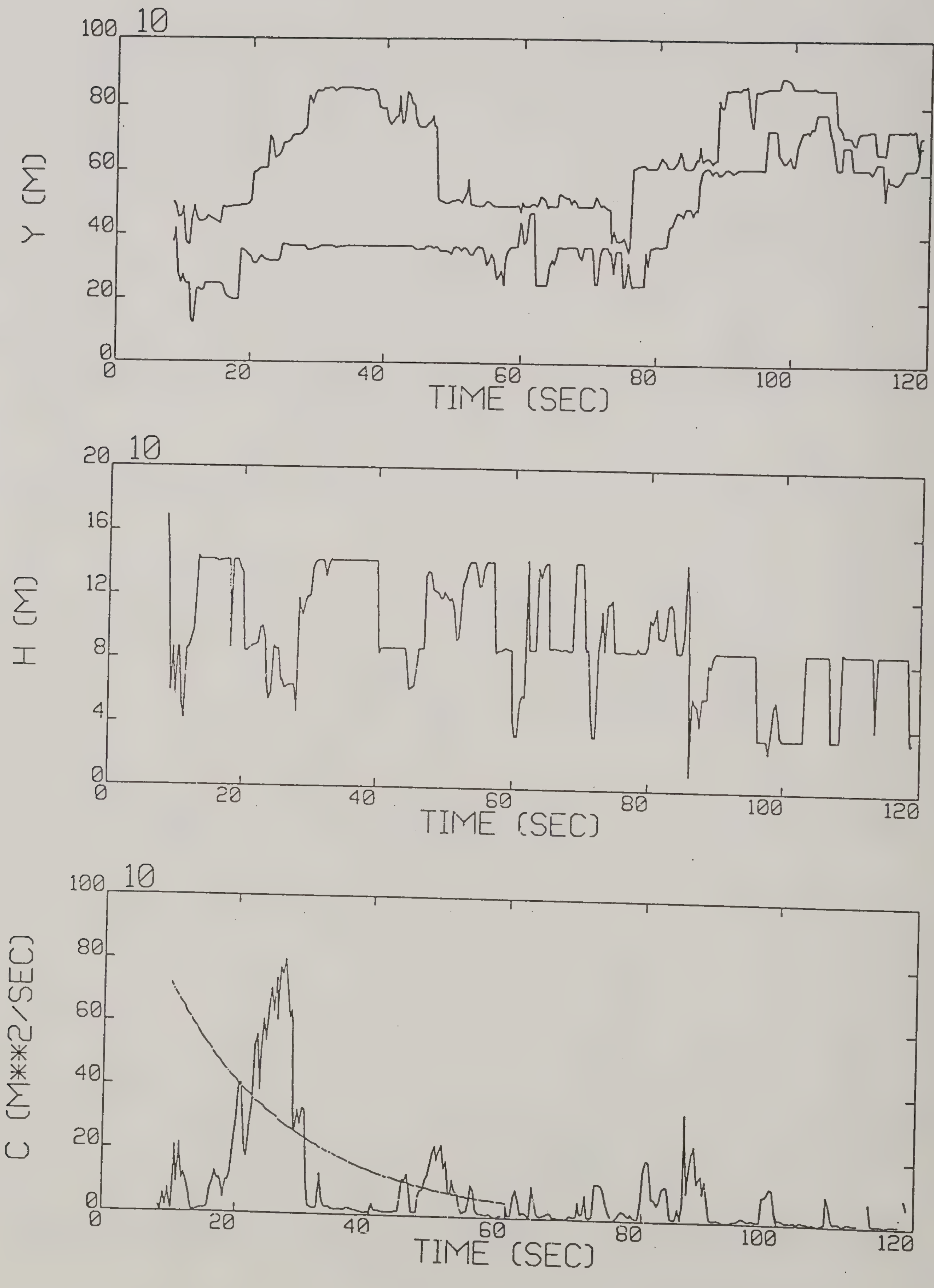

Figure 3-11: Track for run 10 at Dugway.

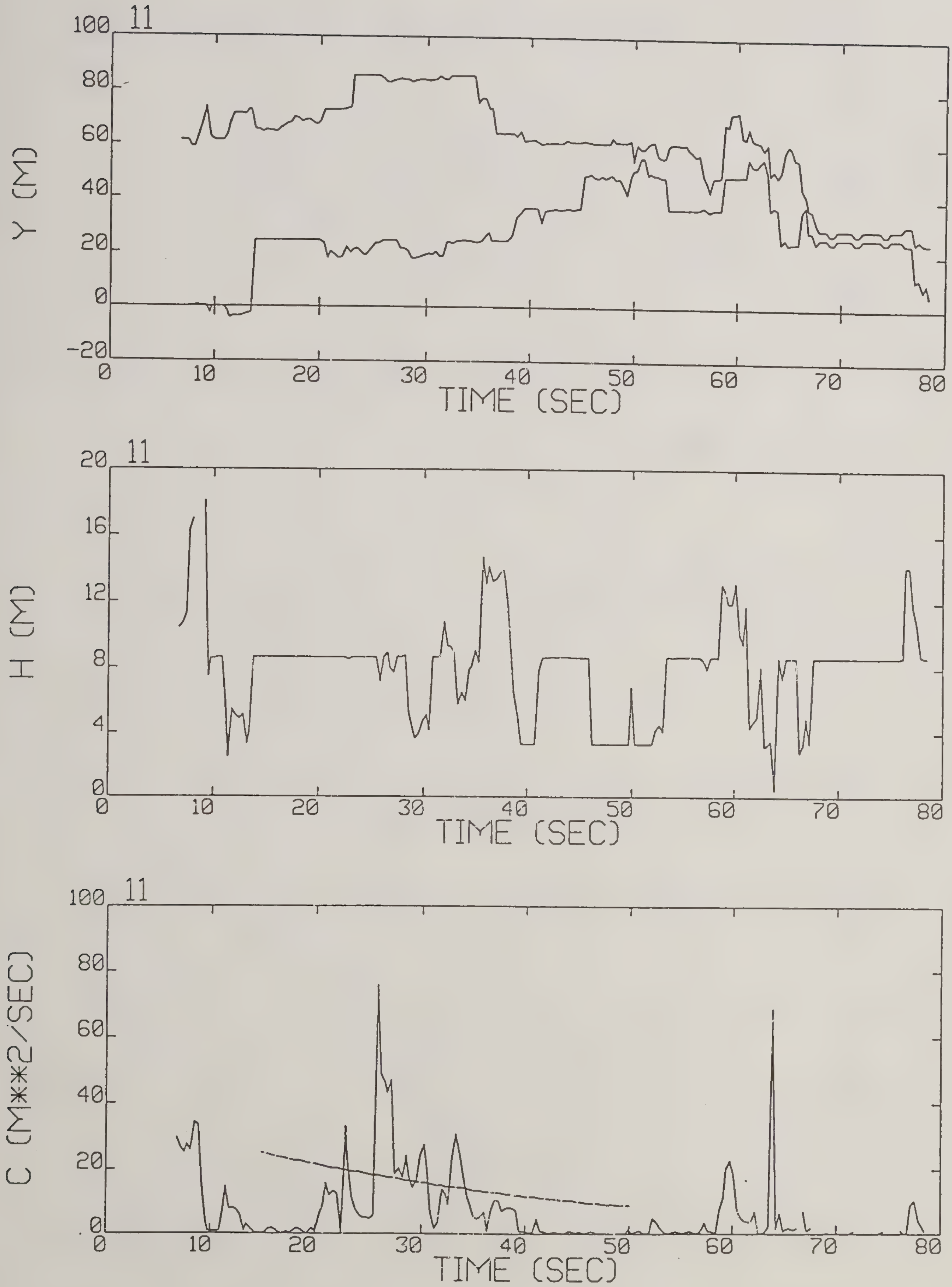

Figure 3-12: Track for run 11 at Dugway.

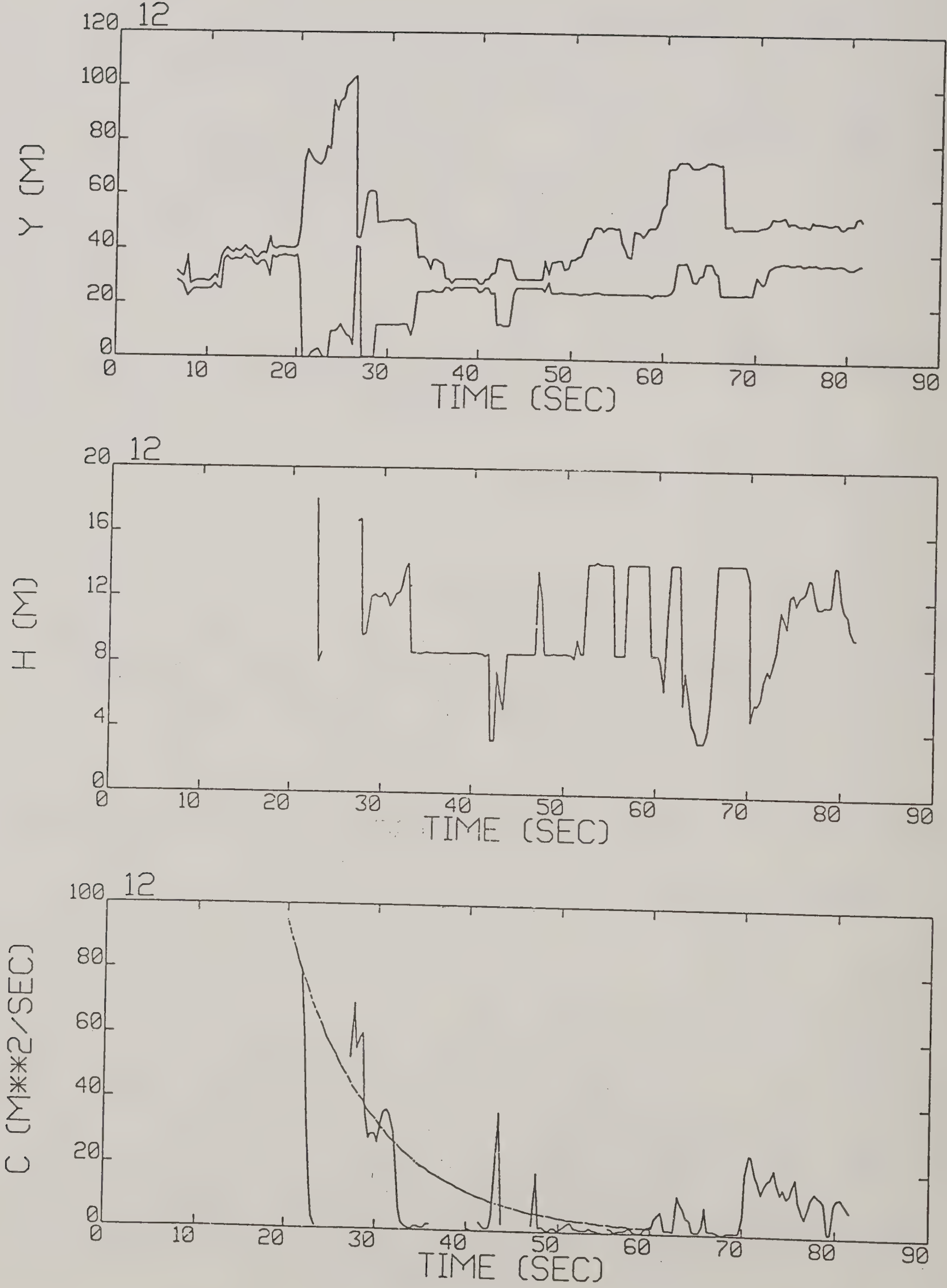

Figure 3-13: Track for run 12 at Dugway.

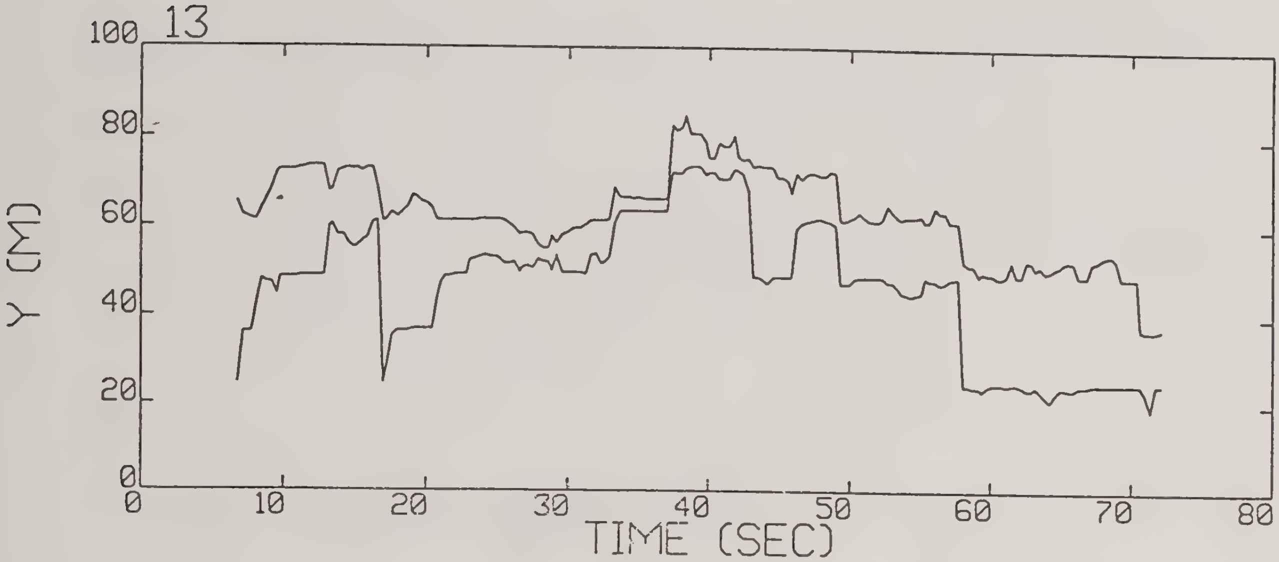

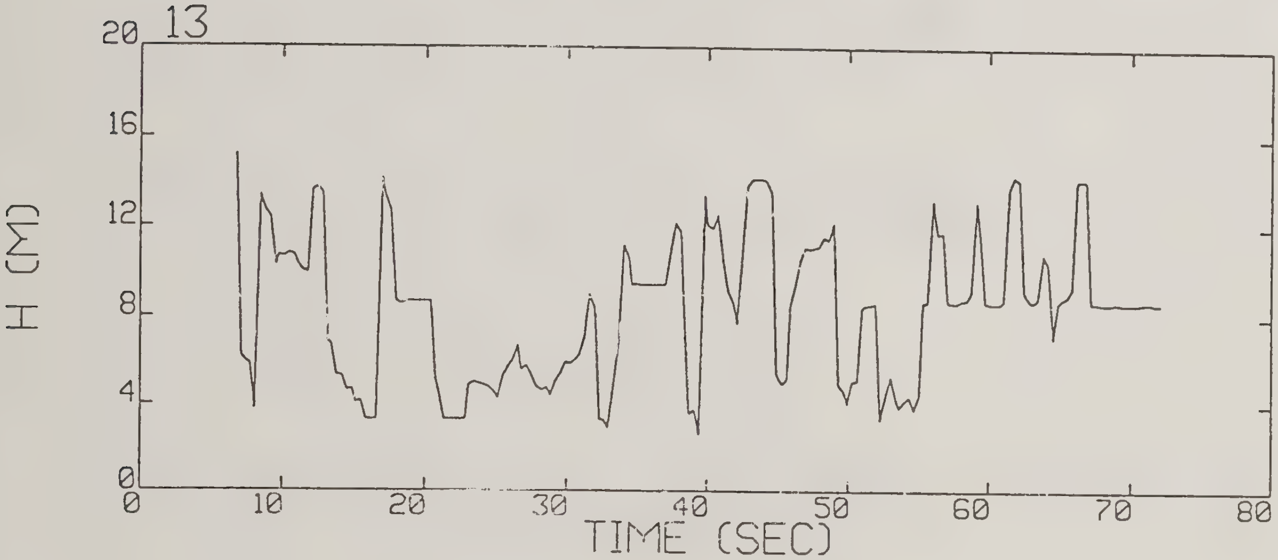

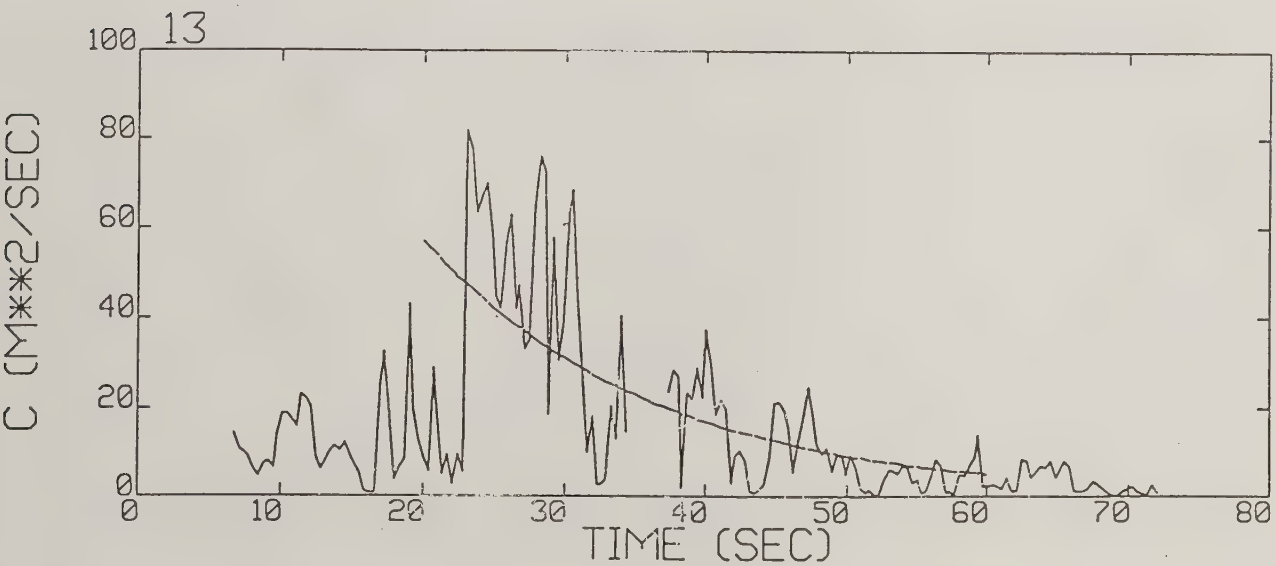

Figure 3-14: Track for run 13 at Dugway.

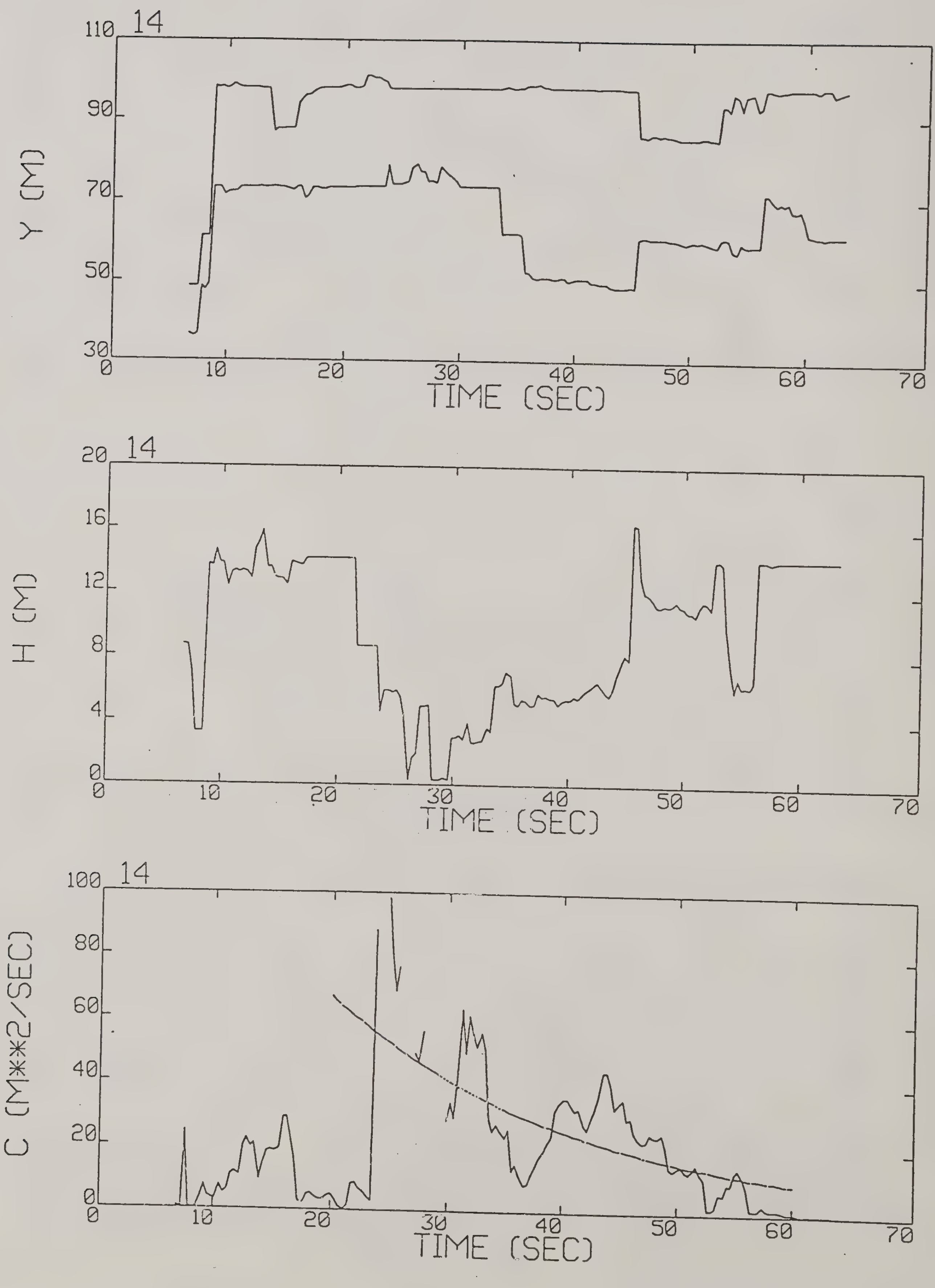

Figure 3-15: Track for run 14 at Dugway.

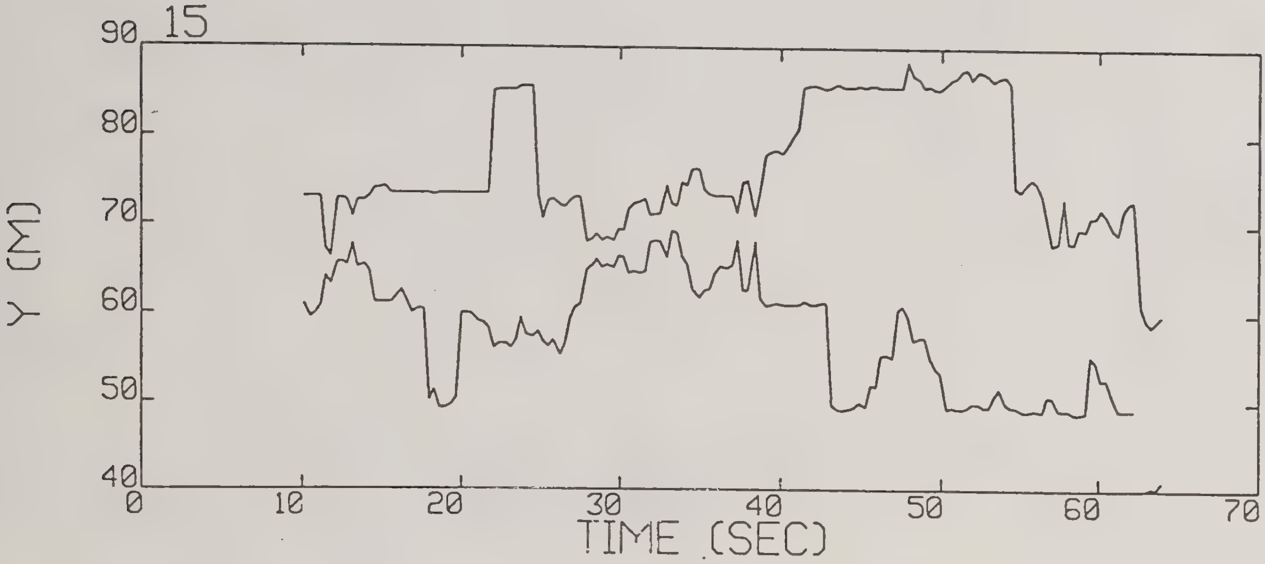

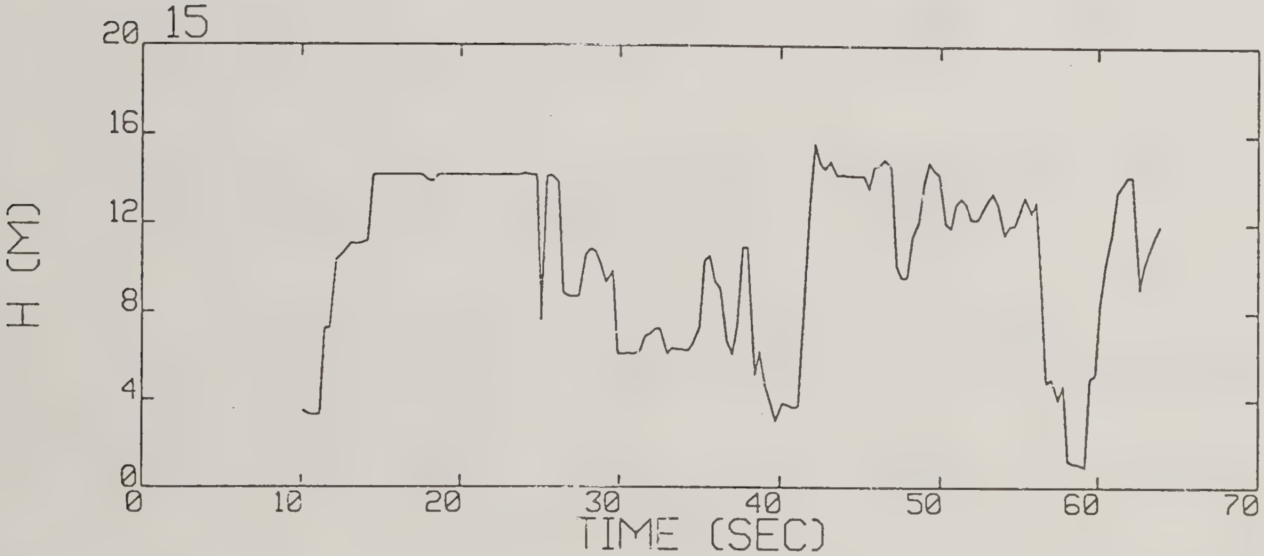

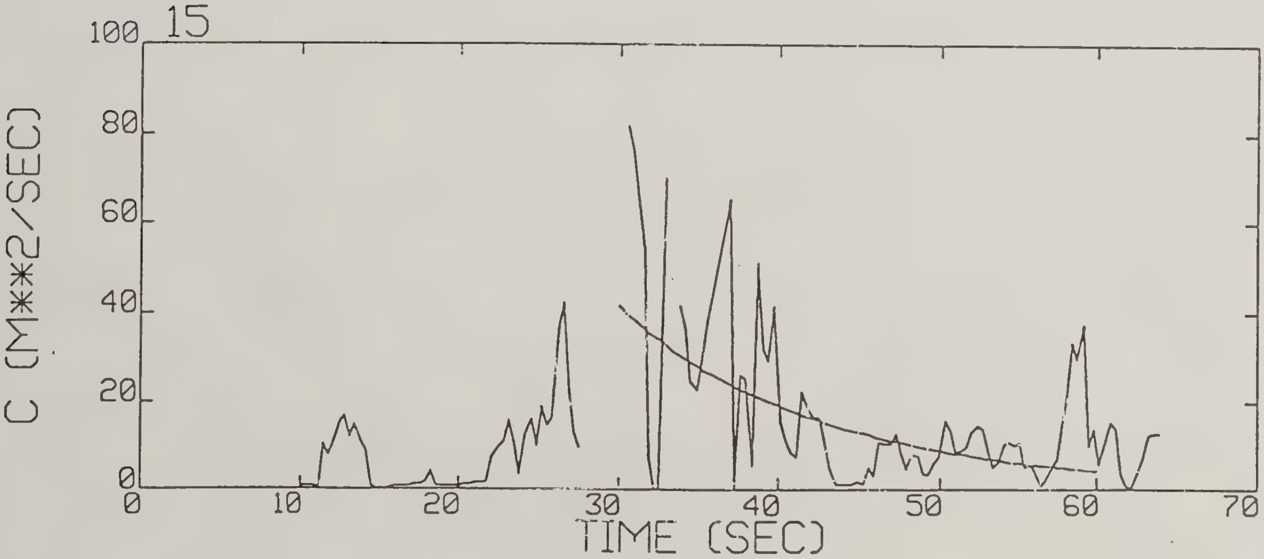

Figure 3-16: Track for run 15 at Dugway.

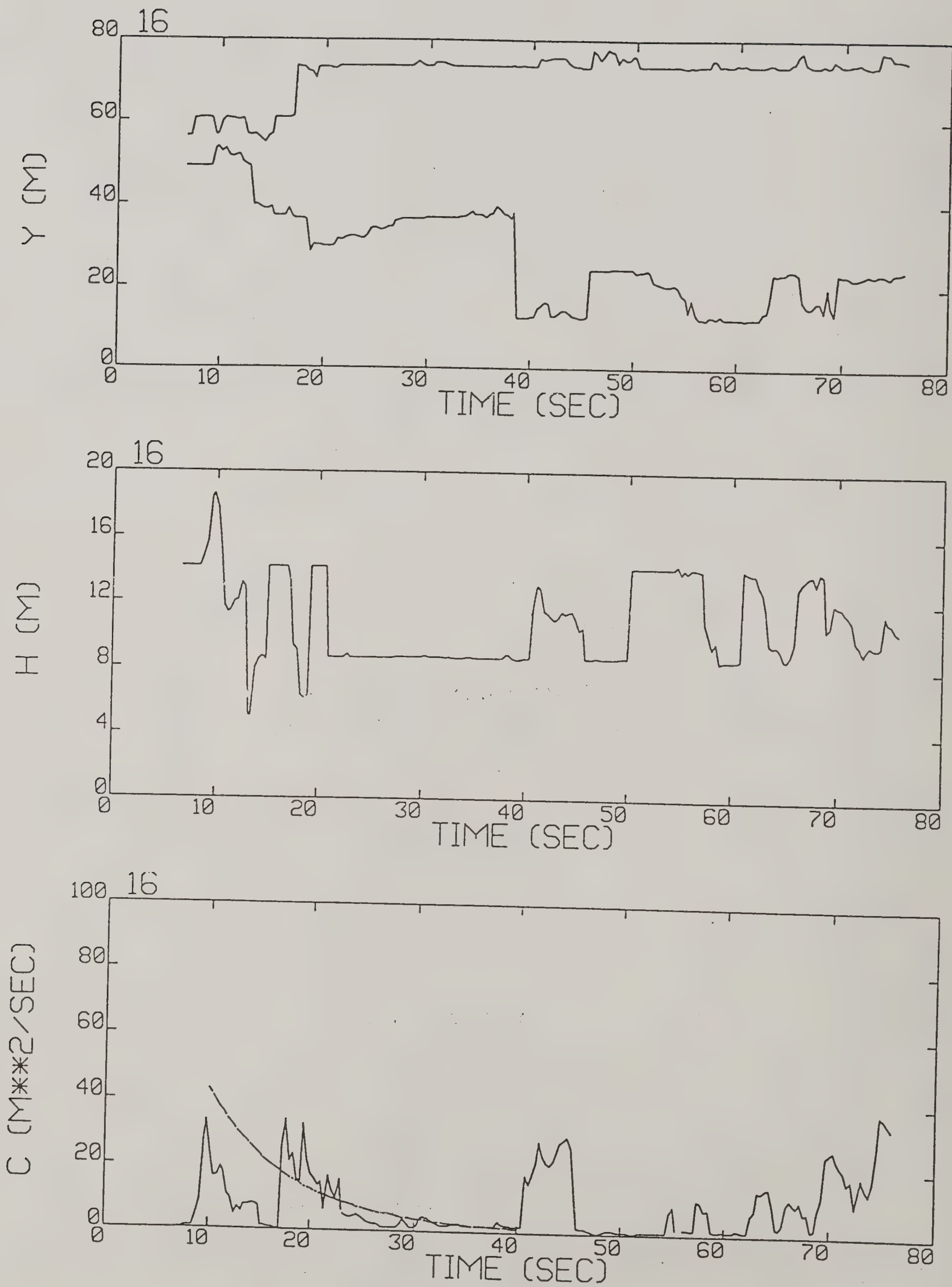

Figure 3-17: Track for run 16 at Dugway.

4. DETERMINATION OF DECAY COEFFICIENT

The vortex strength decay model proposed in Ref. 1 is of the form

$$\Gamma(t) = \Gamma_o \exp\left(- \frac{bqt}{s}\right) \tag{4-1}$$

where

Γ = vortex circulation strength as a function of time t
Γ_o = initial vortex circulation strength at $t = 0$
b = decay coefficient
q = turbulence level
s = vortex pair semispan

This expression was suggested as a possible model for vortex decay in the atmosphere in Ref. 4, with a decay coefficient value estimated to be 0.41 .

Again, a least squares approach was used to curve fit the vortex circulation strength data developed by the generalized algorithm. The vortex circulation strength profiles were fit to Eq. (4-1) by minimizing the logarithmic error

$$E = \sum [G - (A - Bt)]^2 \tag{4-2}$$

over all applicable time increments in each run examined, where

G = logarithm of Γ_i
A = logarithm of Γ_o
B = bq/s
Γ_i = vortex circulation strength generalized algorithm values

Equation (4-2) returns the best fit values for Γ_o and B for each run examined (comparisons were shown in Figures 3-3 to 3-17 above). Since the semispan s was known, the value of B could be used to infer the product bq for each run examined.

The first five seconds of each run could then be quizzed for the U and V horizontal wind velocities at the two U-V-W anemometers. This data is shown in Figures 4-1 to 4-15, and is used to estimate the turbulence level q for each run by a least squares curve fit to a neutral logarithmic profile of the form

$$U = U_o \ln (z/z_o) \qquad (4\text{-}3)$$

where

U = horizontal surface velocity
U_o = reference velocity
z = reference height
z_o = surface roughness

A consistent turbulence level may then be obtained by using an equation found in Ref. 2

$$q^2 = 0.845\, U_o^2 \qquad (4\text{-}4)$$

With the turbulence level q determined, the product bq may be plotted as shown in Figure 4-16. Here it may be seen that bq is approximated by its average value of 0.56 m/sec and standard deviation of 0.32 m/sec, as determined with the Program WIND data (Ref. 1). The Dugway data may be seen to be consistent with this data, although the mean of the filled squares in Figure 4-16 appears slightly higher than 0.56 m/sec.

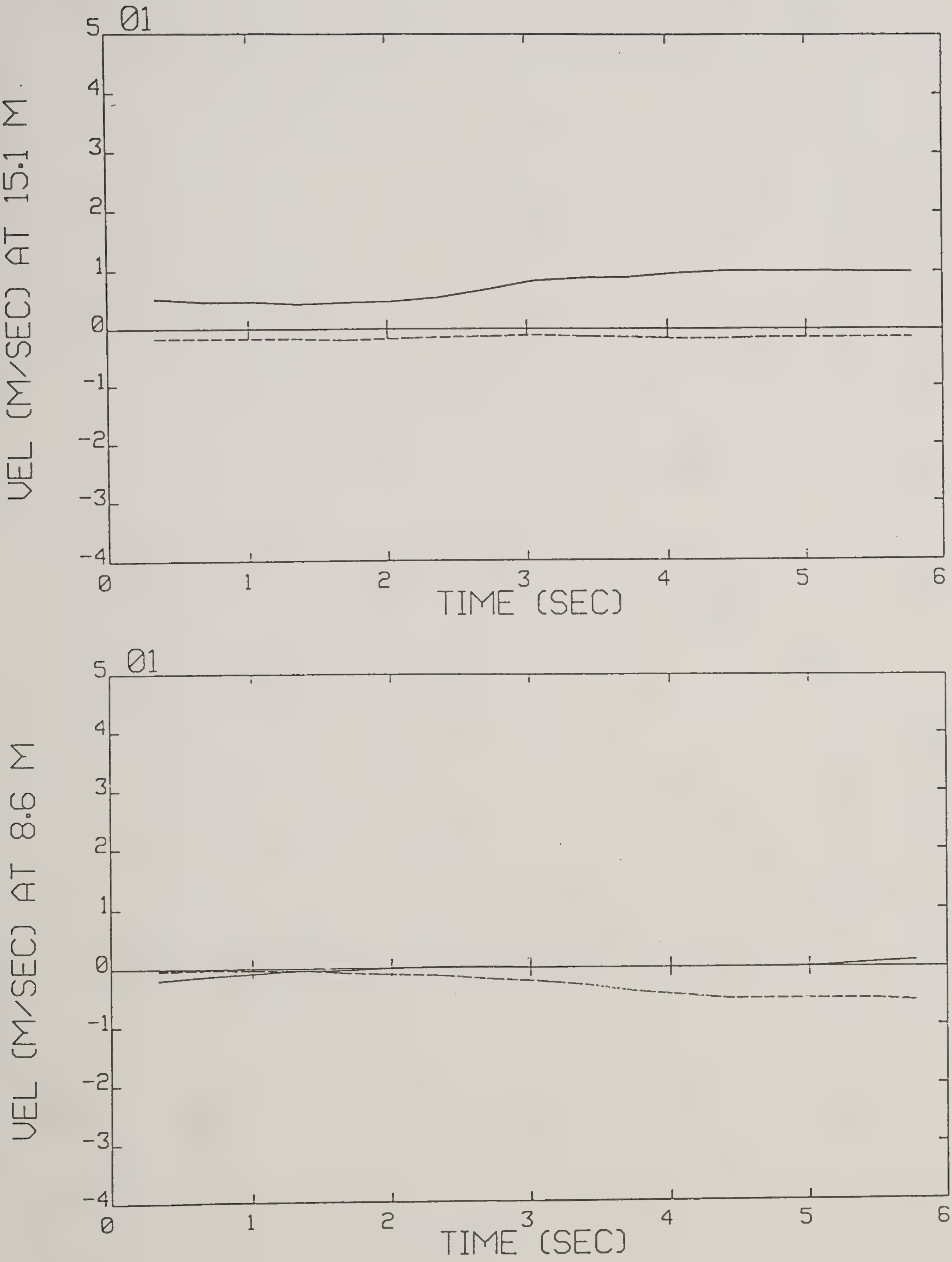

Figure 4-1: Horizontal velocities at the beginning of run 1 at Dugway: U velocity normal to tower grid (solid); V velocity parallel to tower grid (dashed); tower 0 at 15.1 m (top); tower 9 at 8.6 m (bottom).

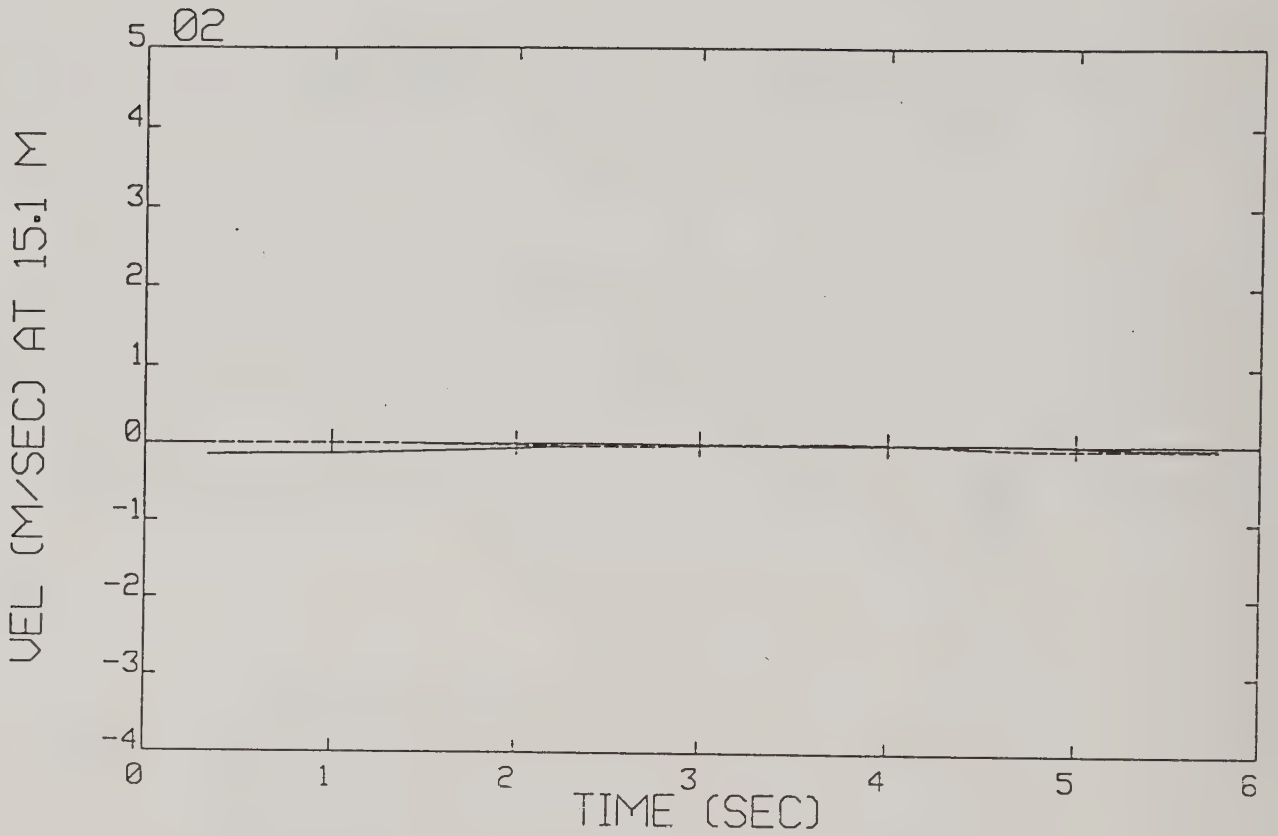

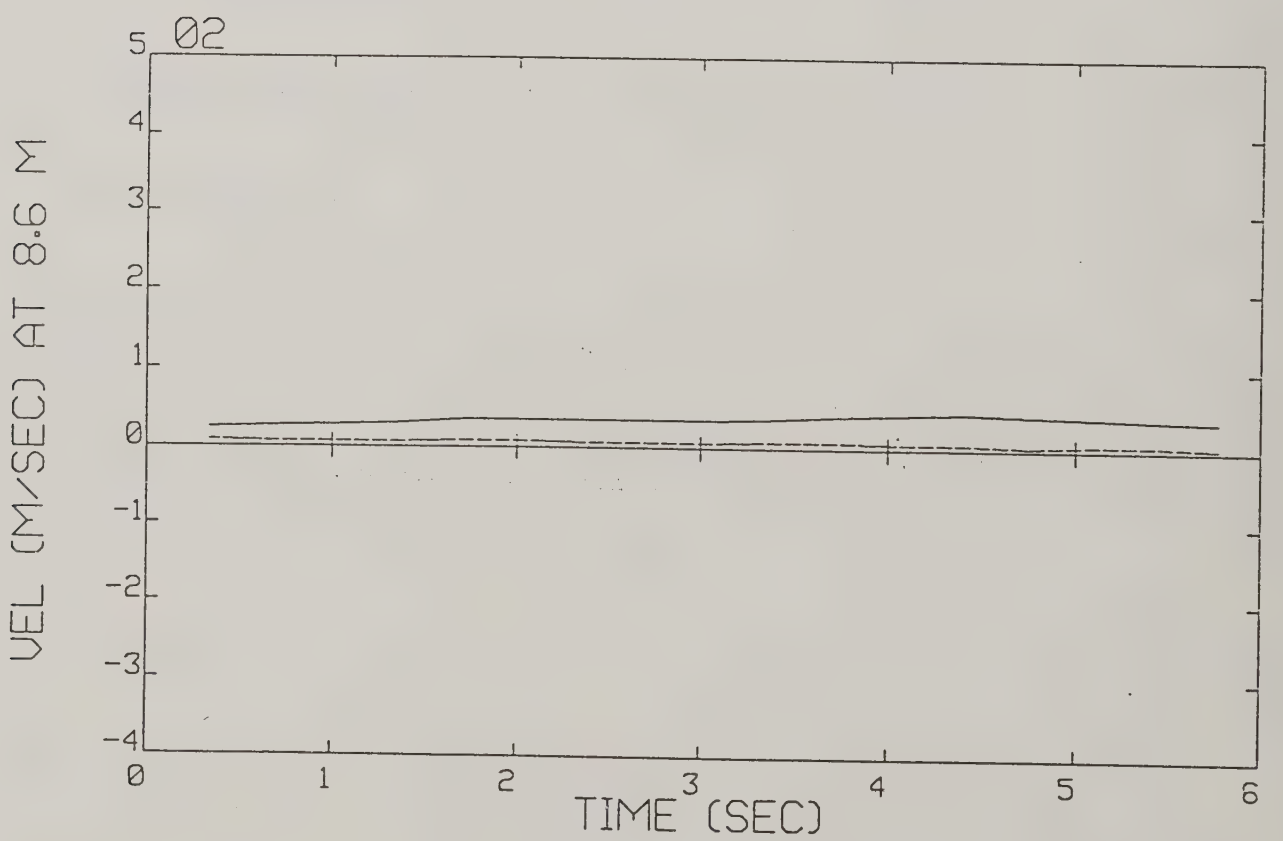

Figure 4-2: Velocities for run 2 at Dugway.

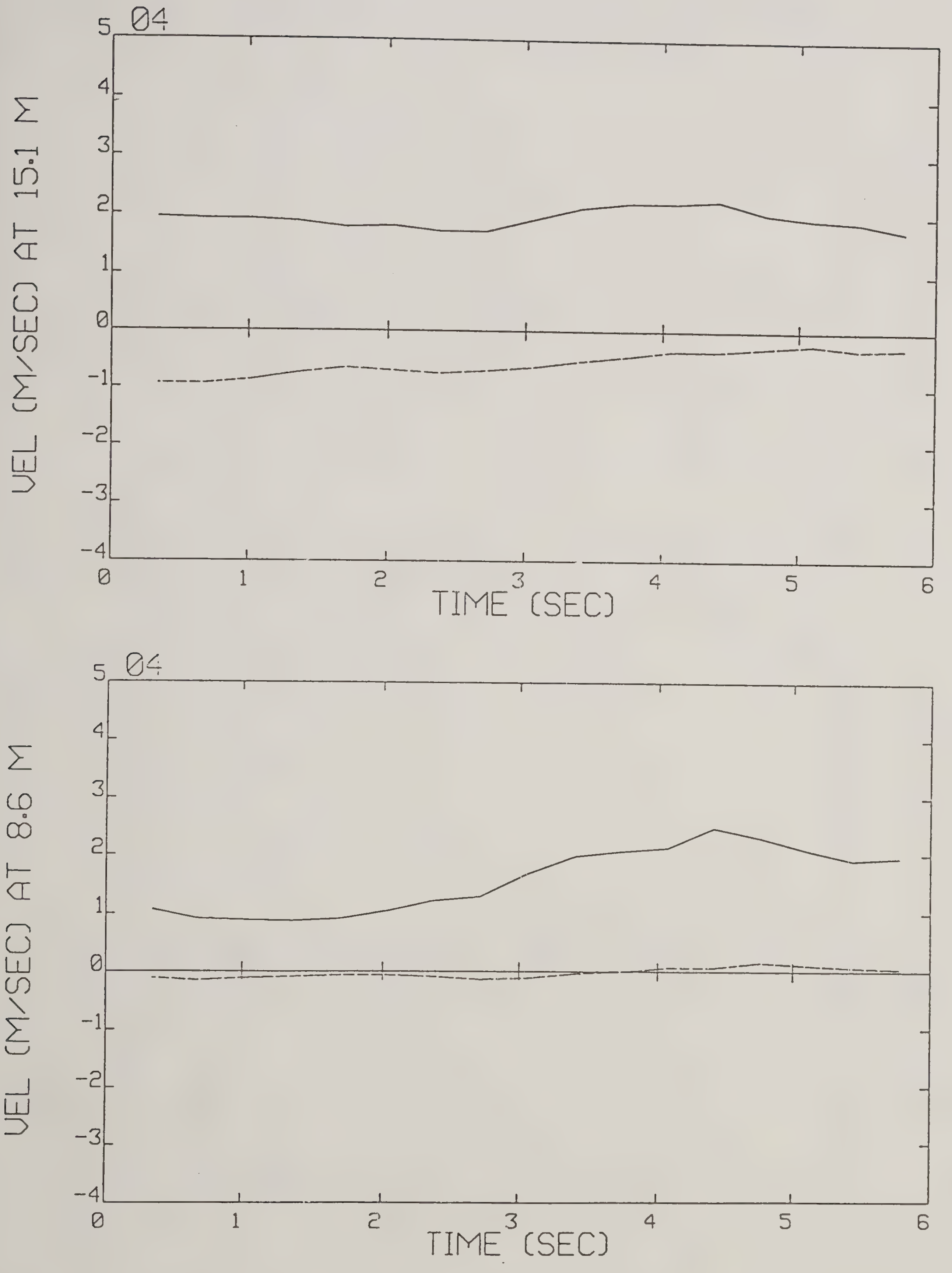

Figure 4-3: Velocities for run 4 at Dugway.

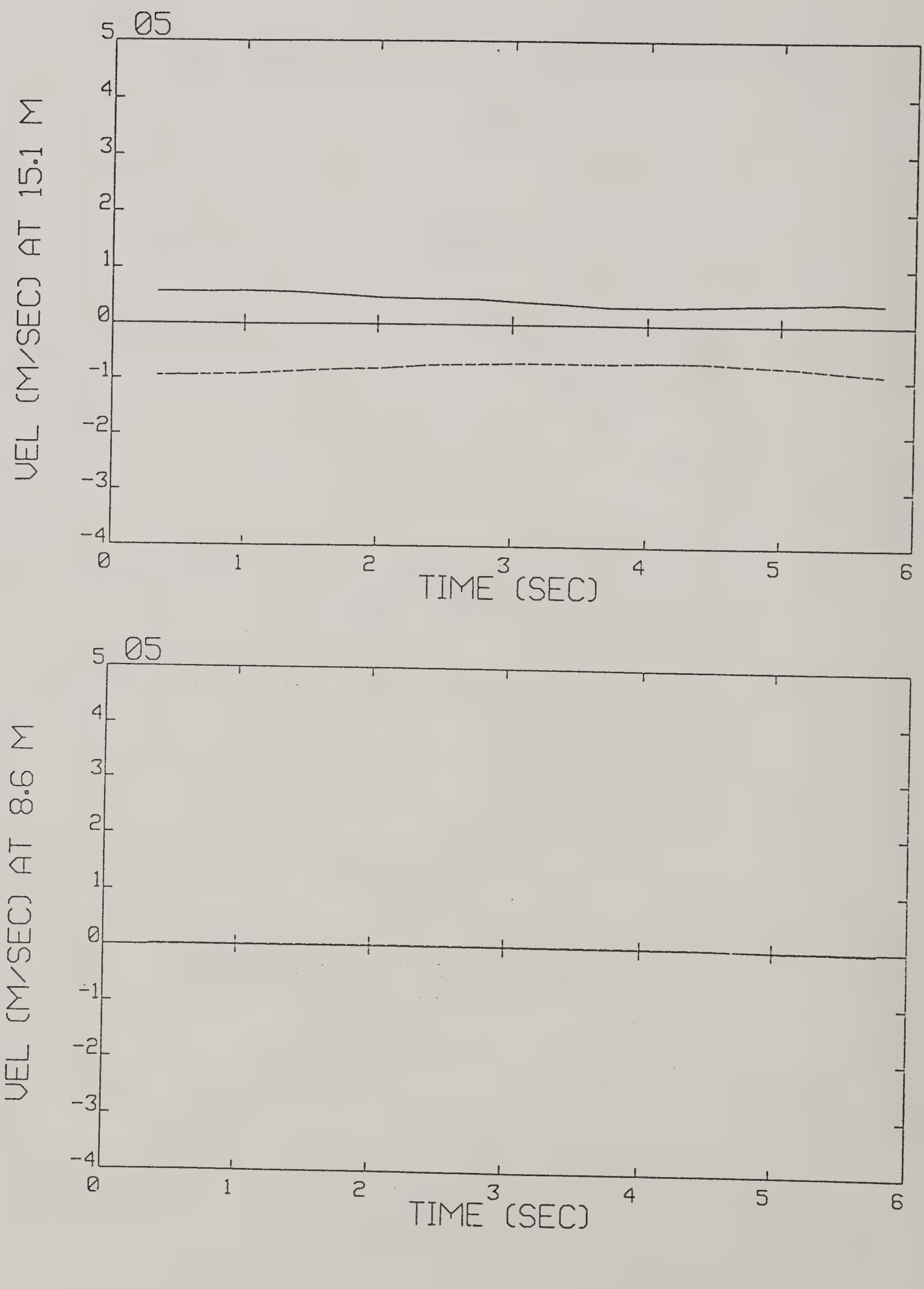

Figure 4-4: Velocities for run 5 at Dugway.

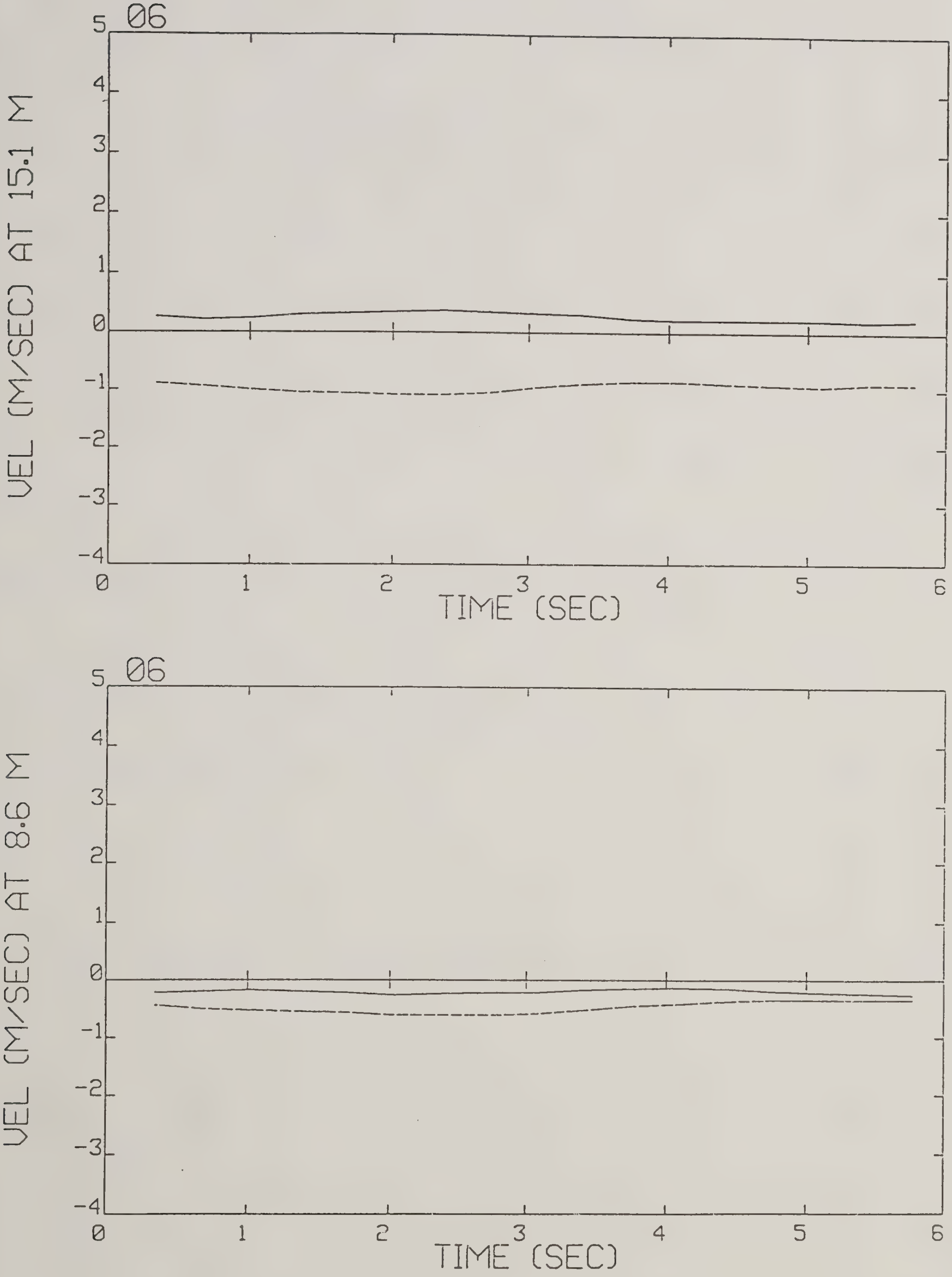

Figure 4-5: Velocities for run 6 at Dugway.

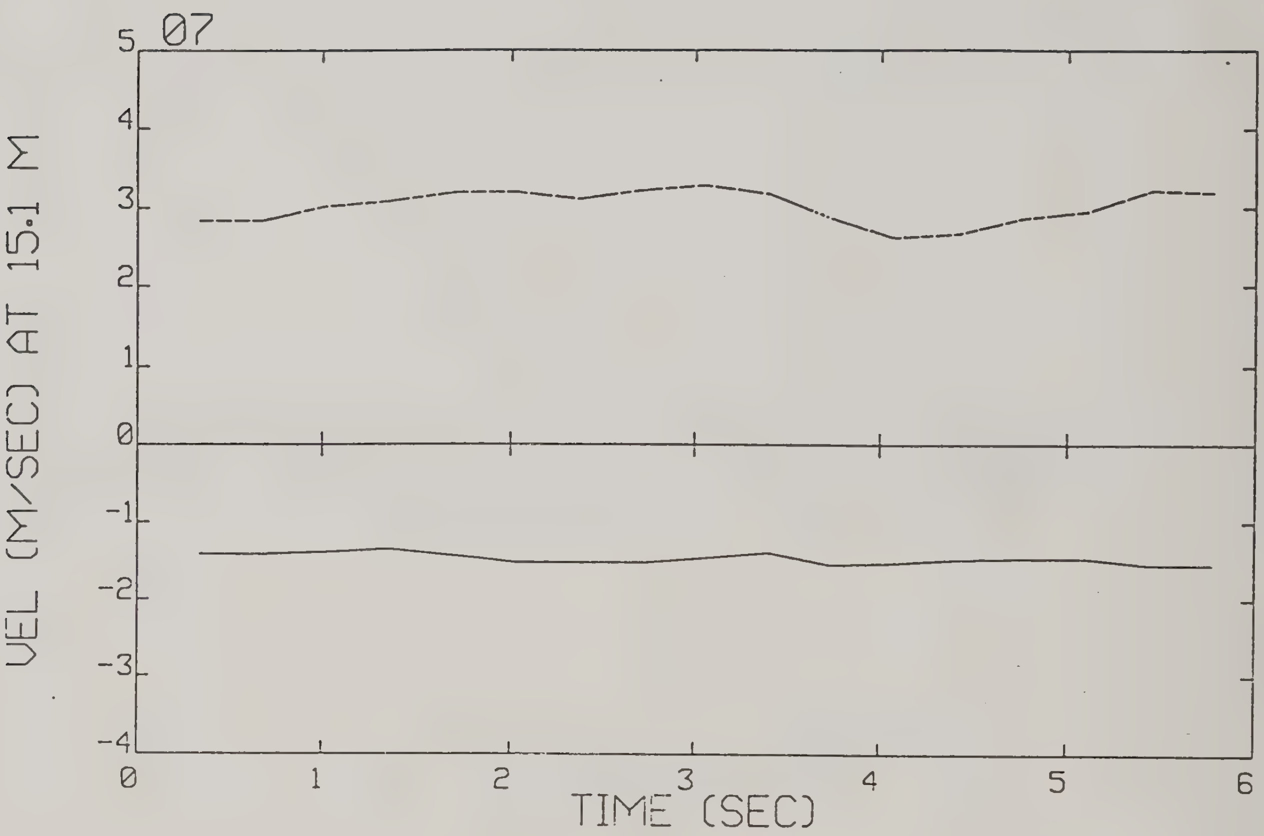

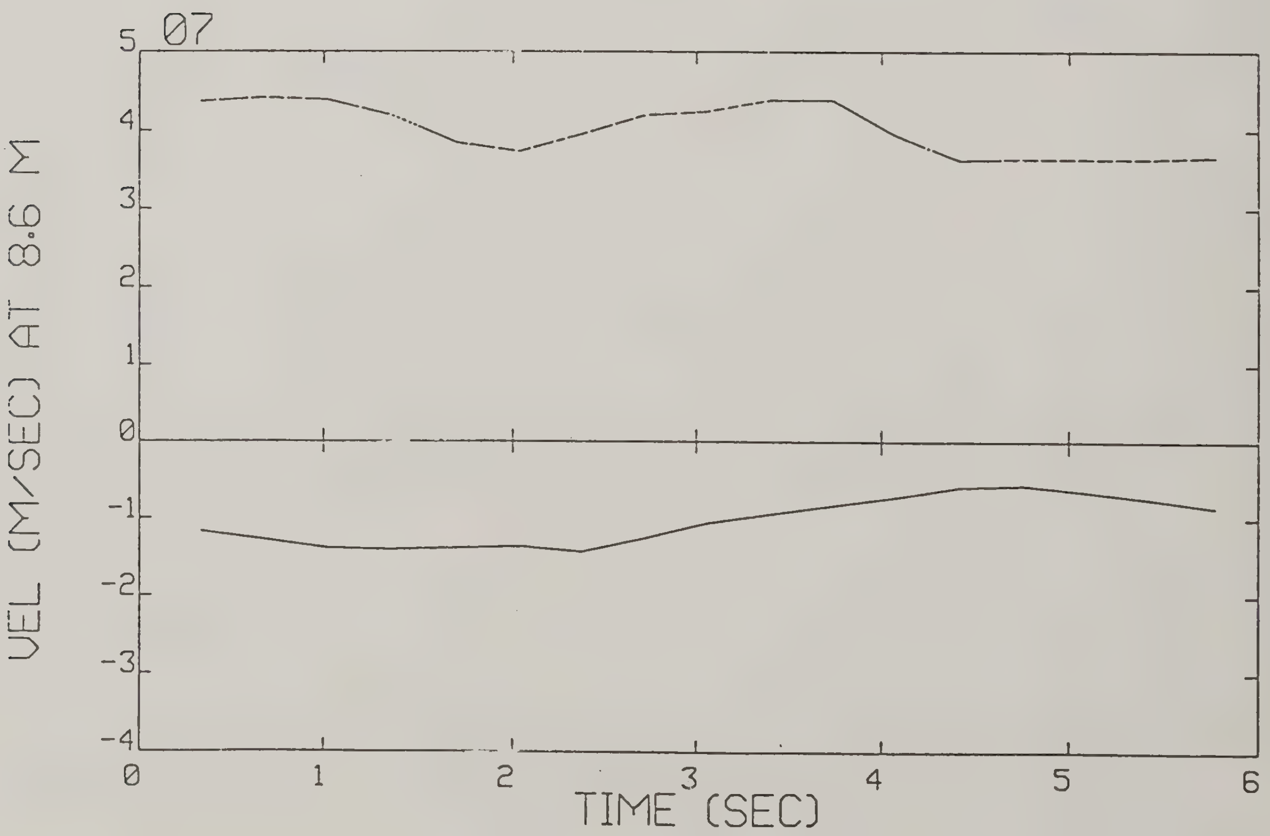

Figure 4-6: Velocities for run 7 at Dugway.

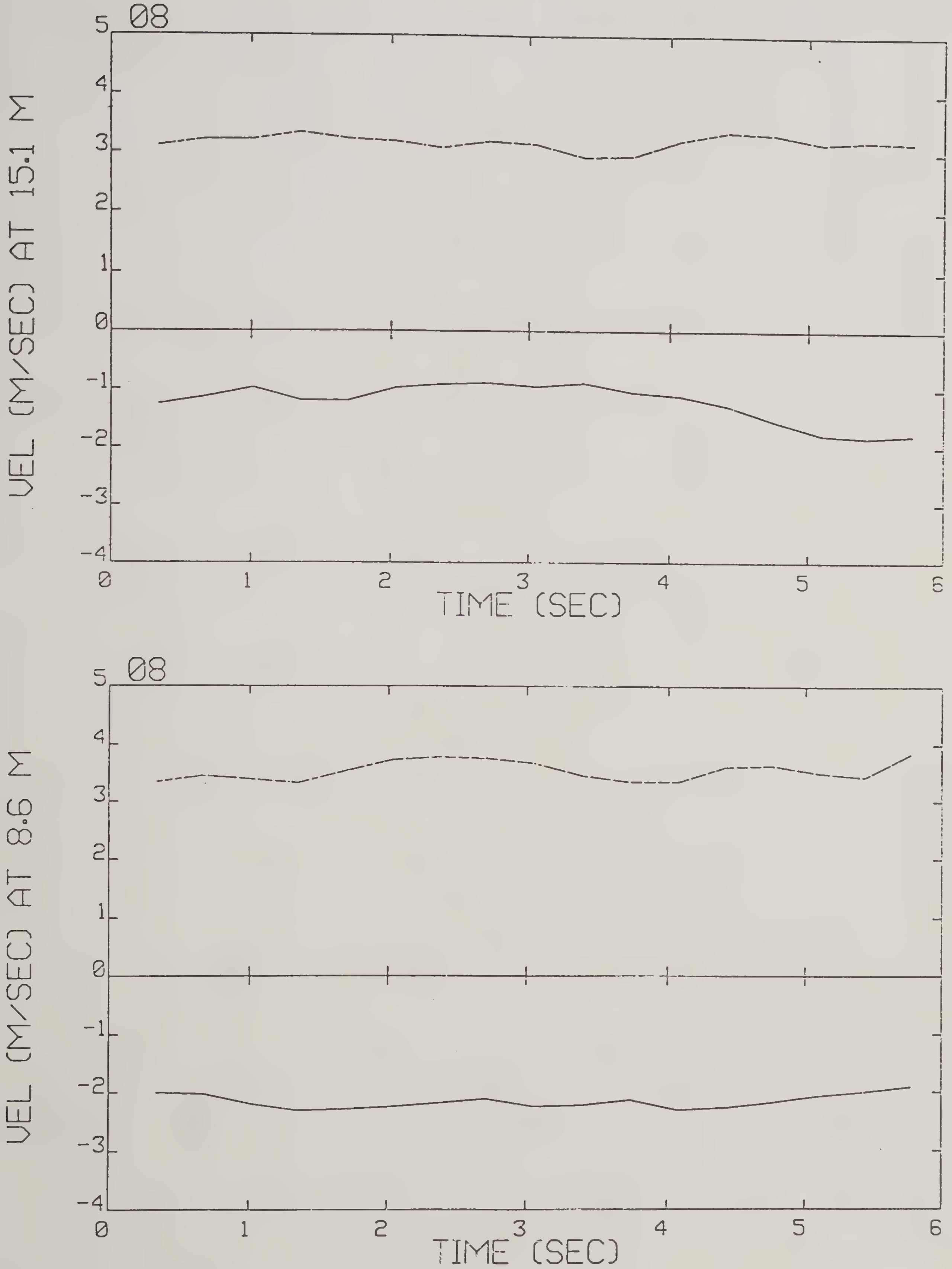

Figure 4-7: Velocities for run 8 at Dugway.

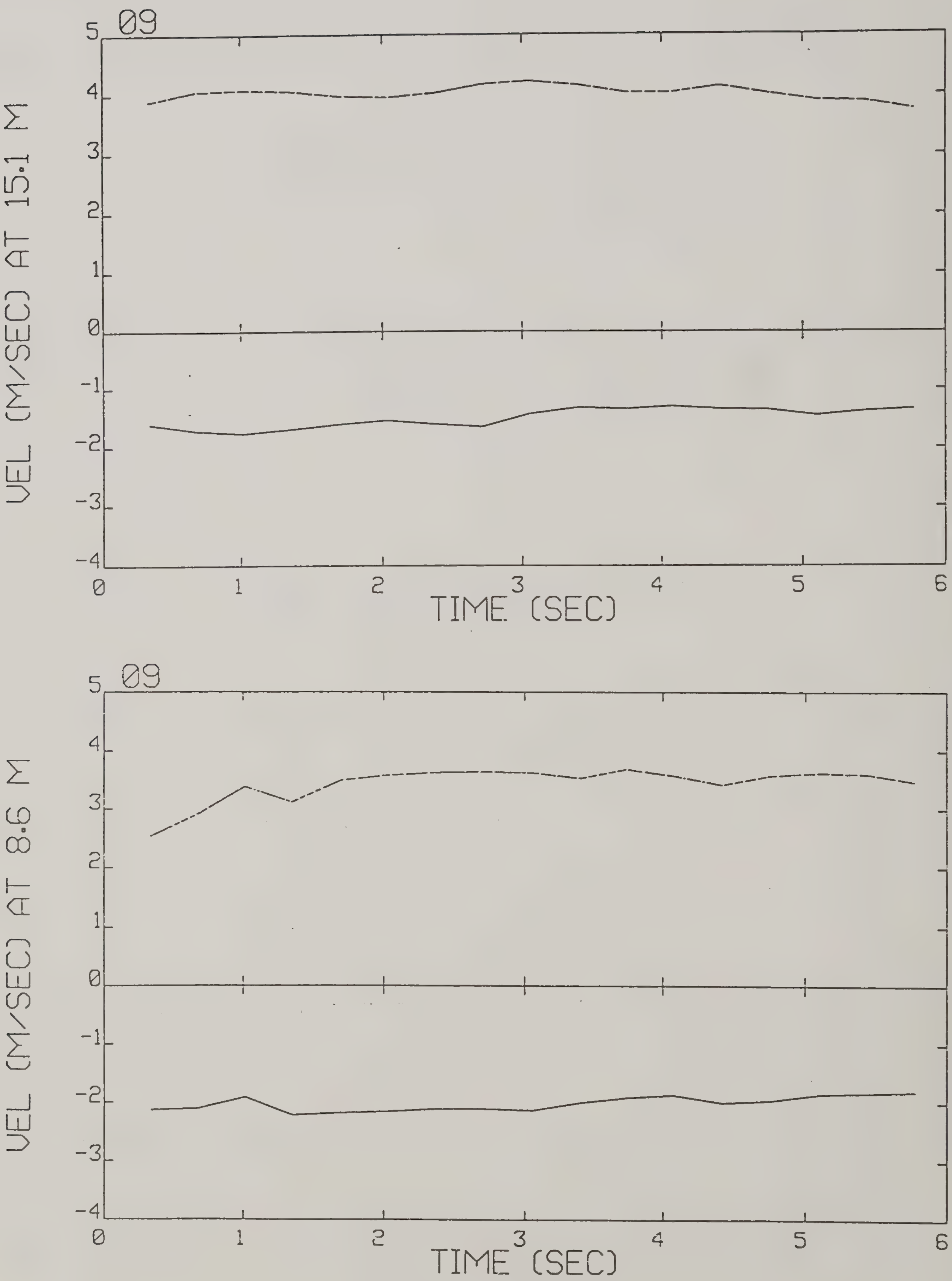

Figure 4-8: Velocities for run 9 at Dugway.

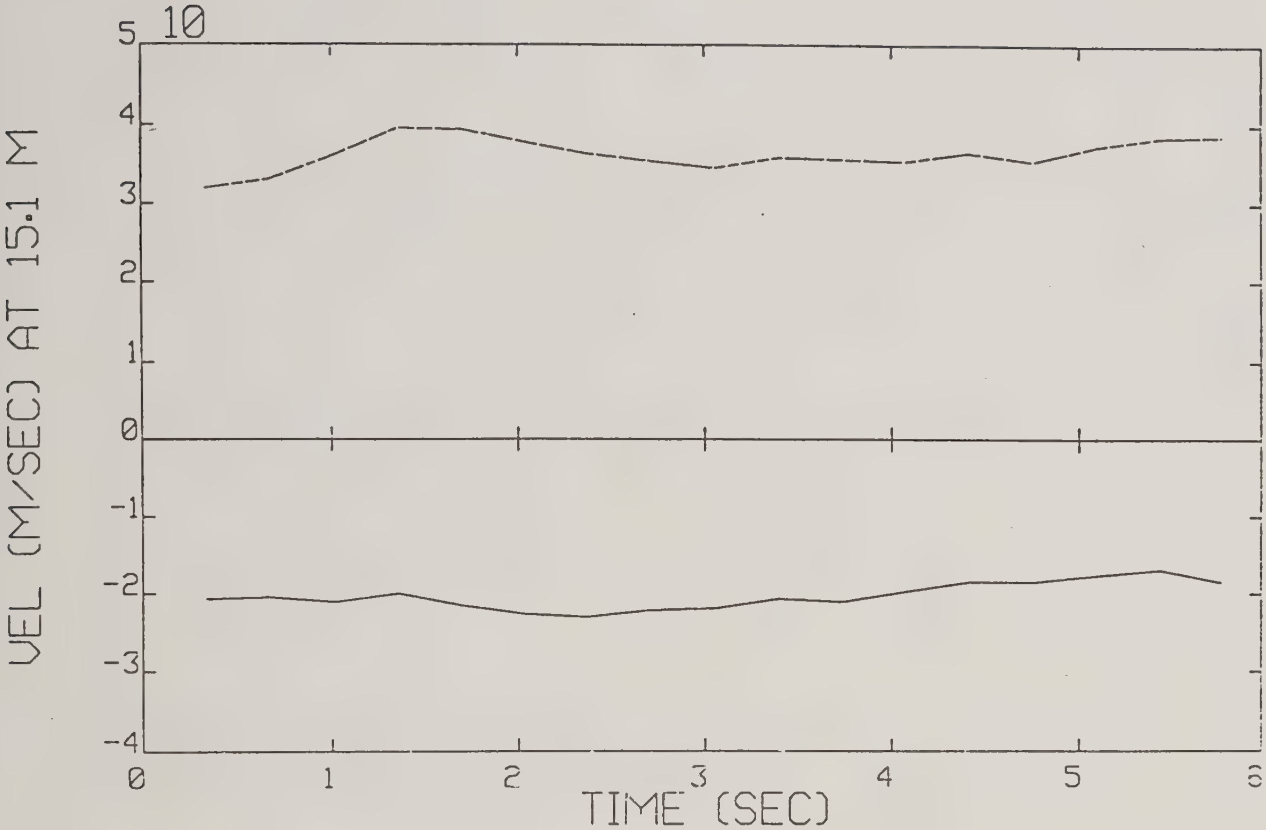

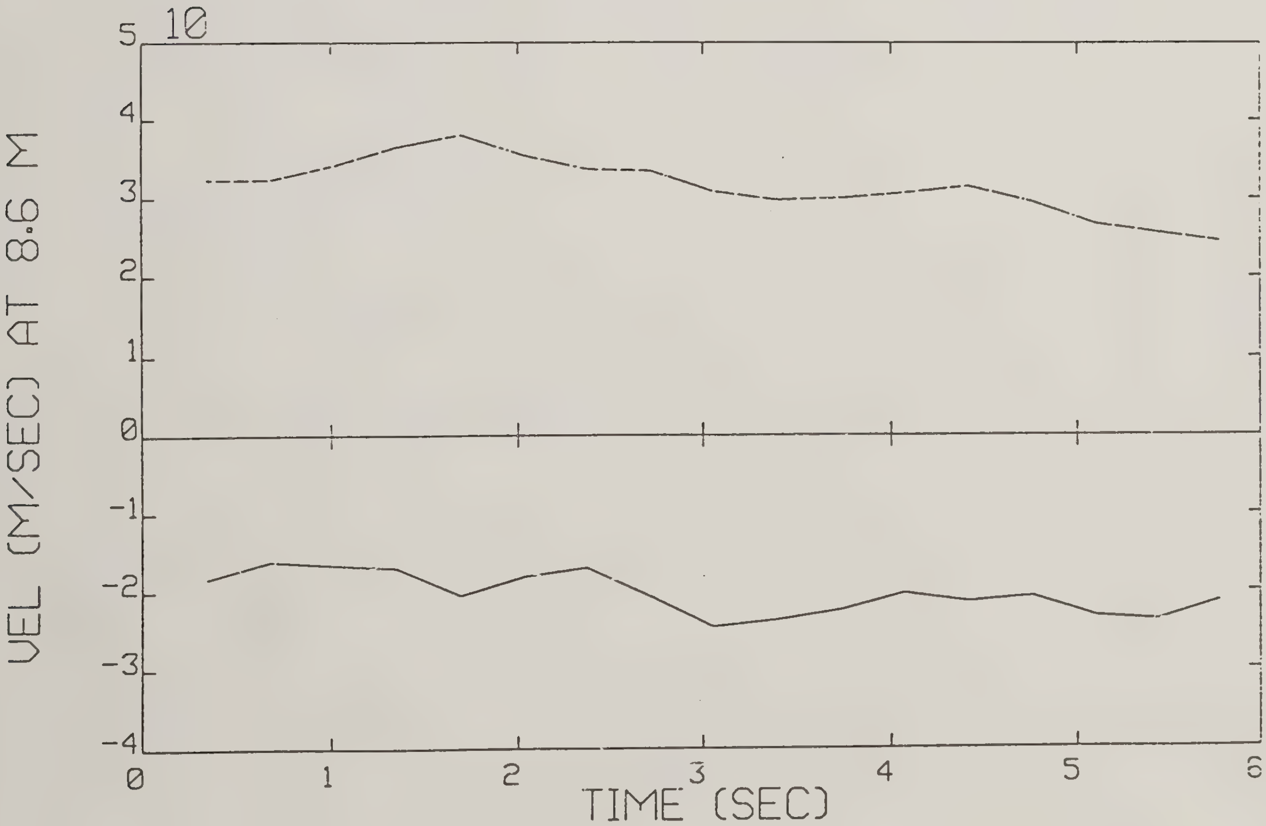

Figure 4-9: Velocities for run 10 at Dugway.

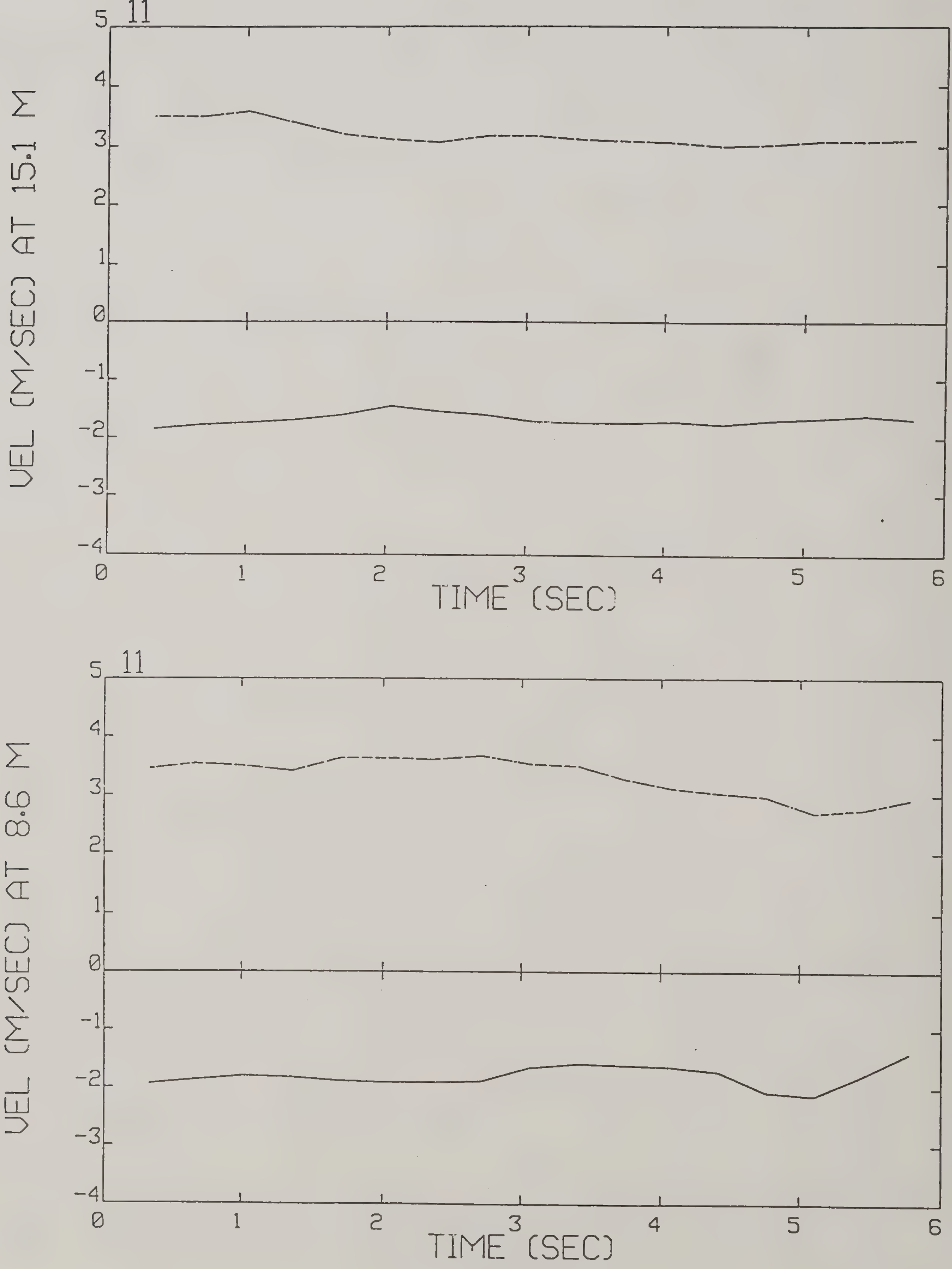

Figure 4-10: Velocities for run 11 at Dugway.

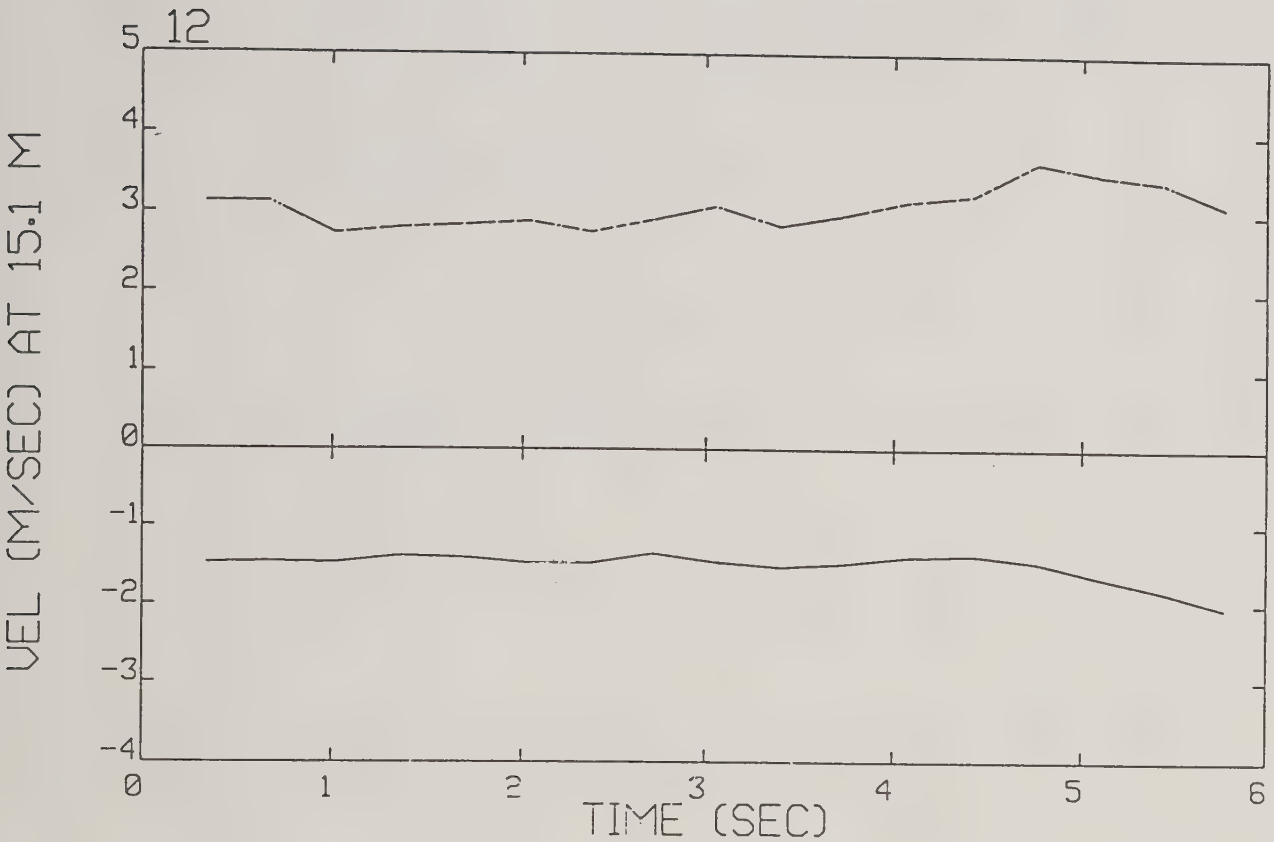

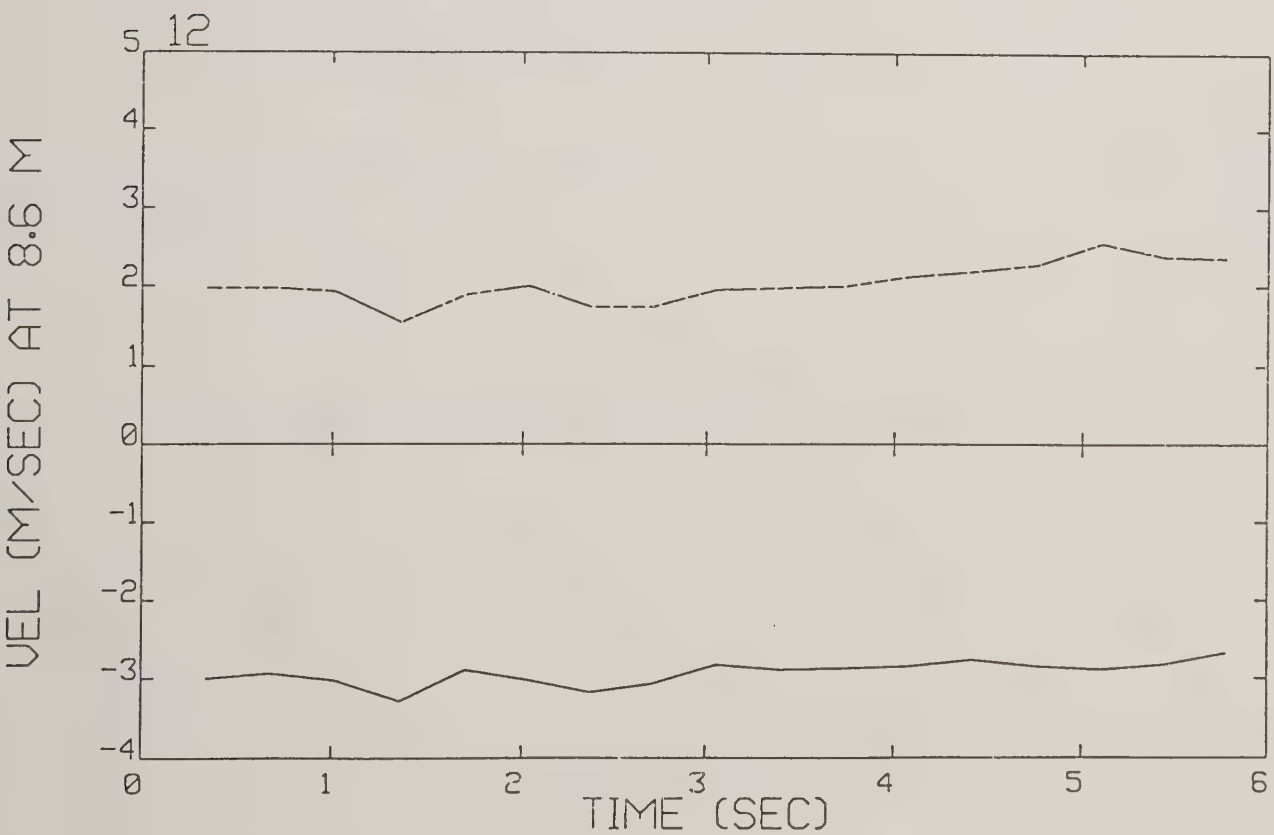

Figure 4-11: Velocities for run 12 at Dugway.

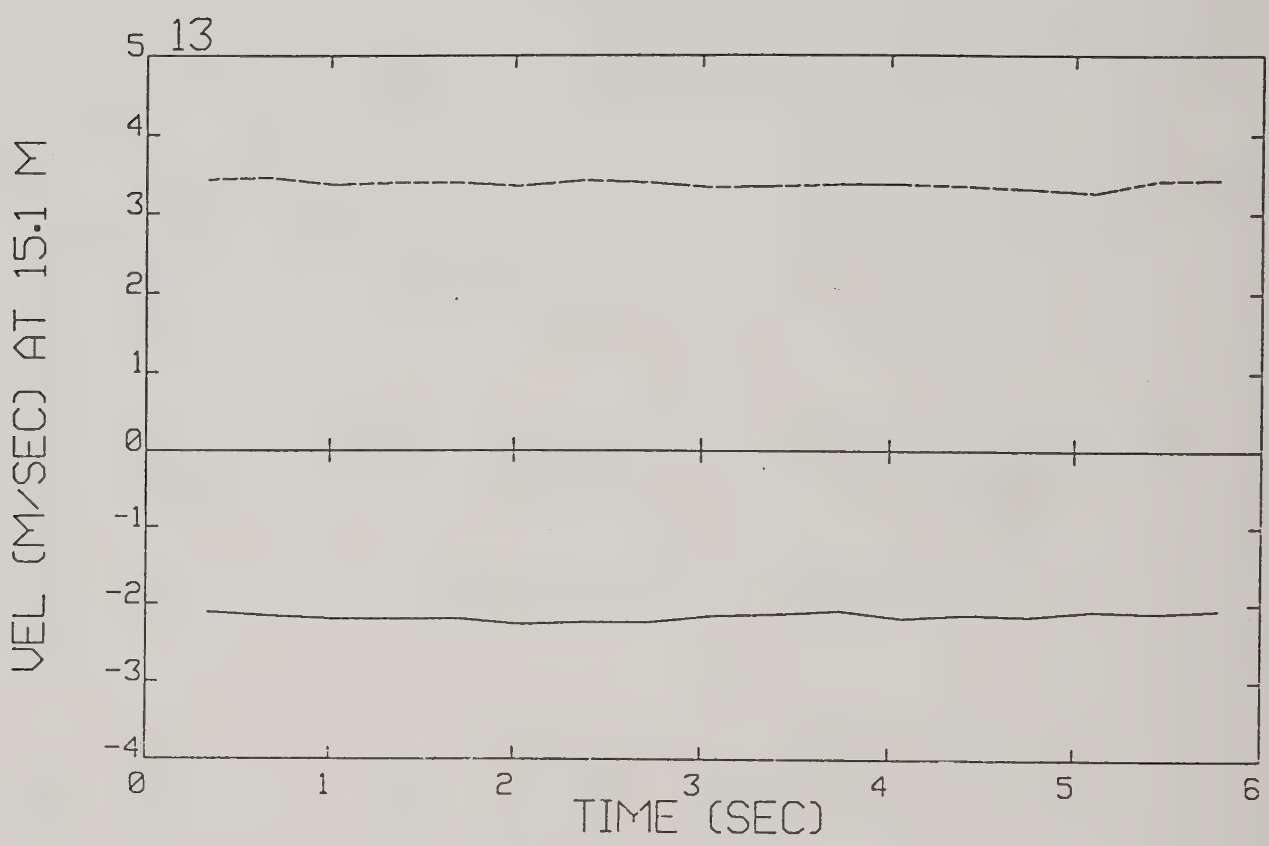

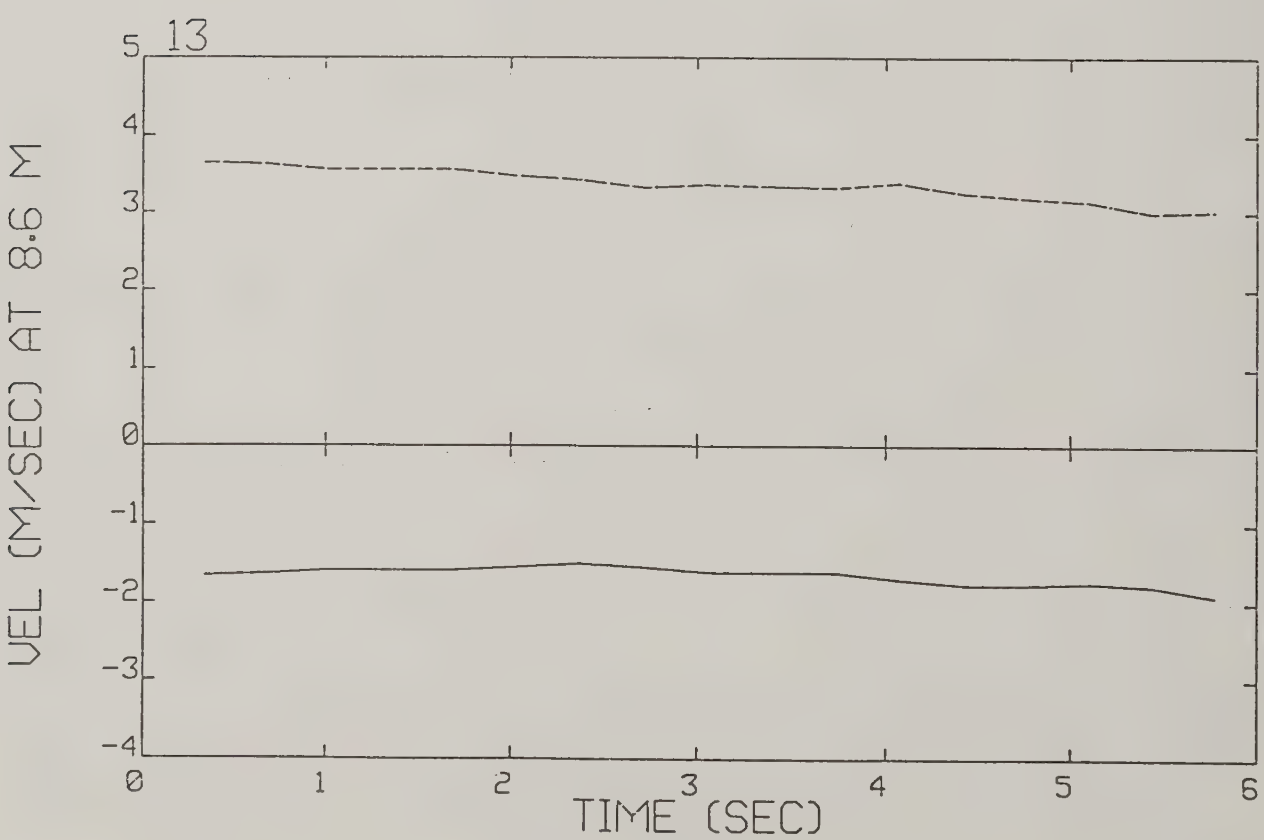

Figure 4-12: Velocities for run 13 at Dugway.

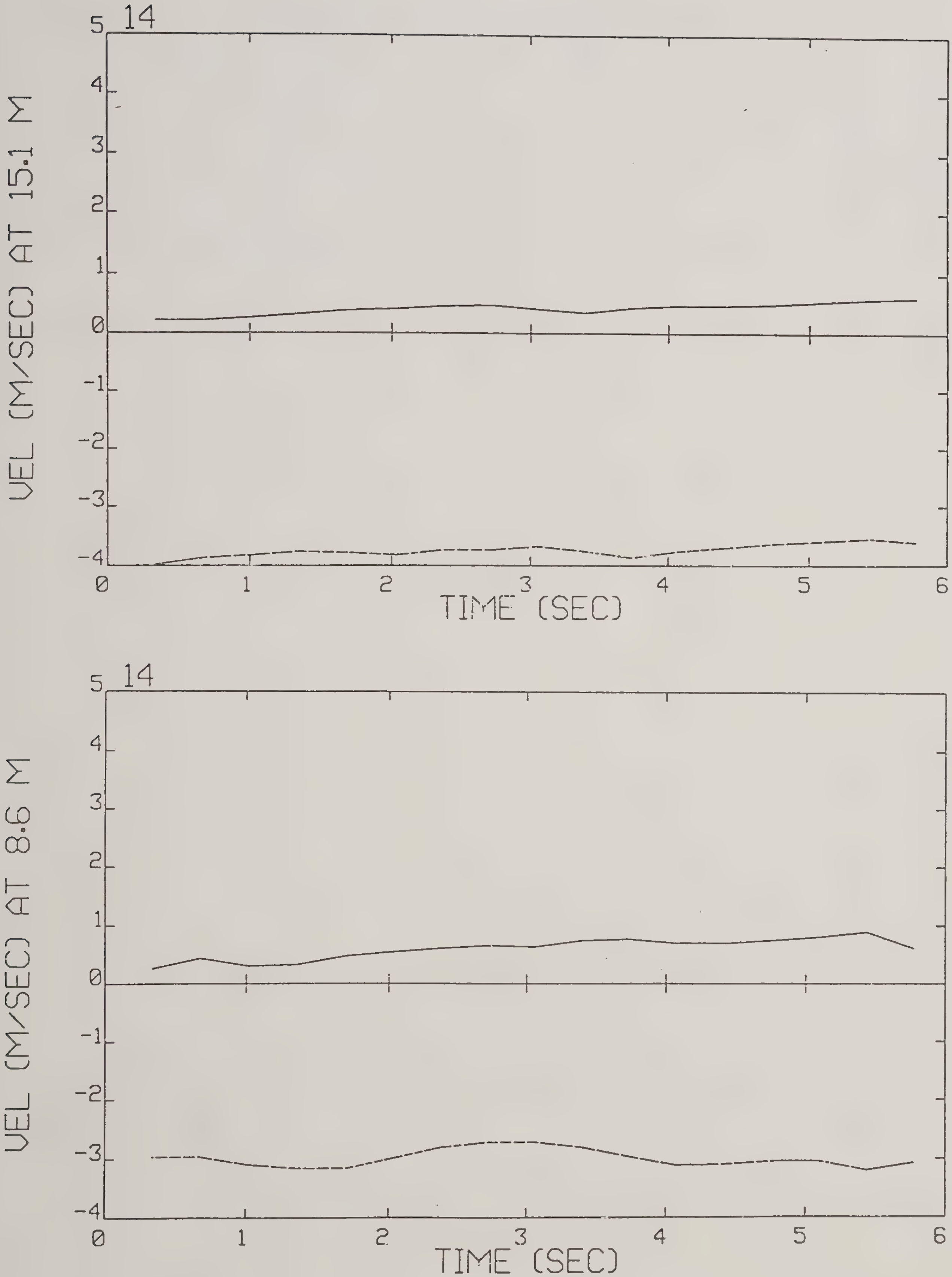

Figure 4-13: Velocities for run 14 at Dugway.

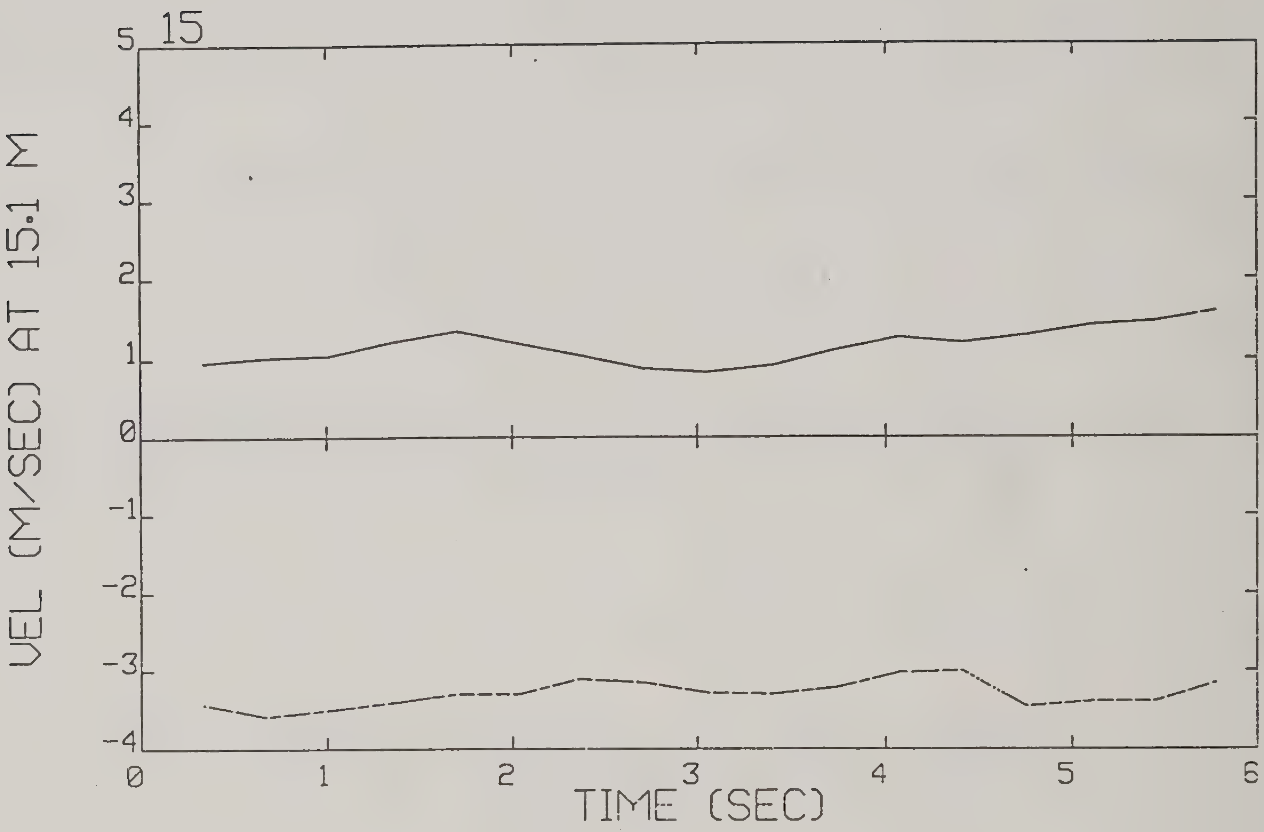

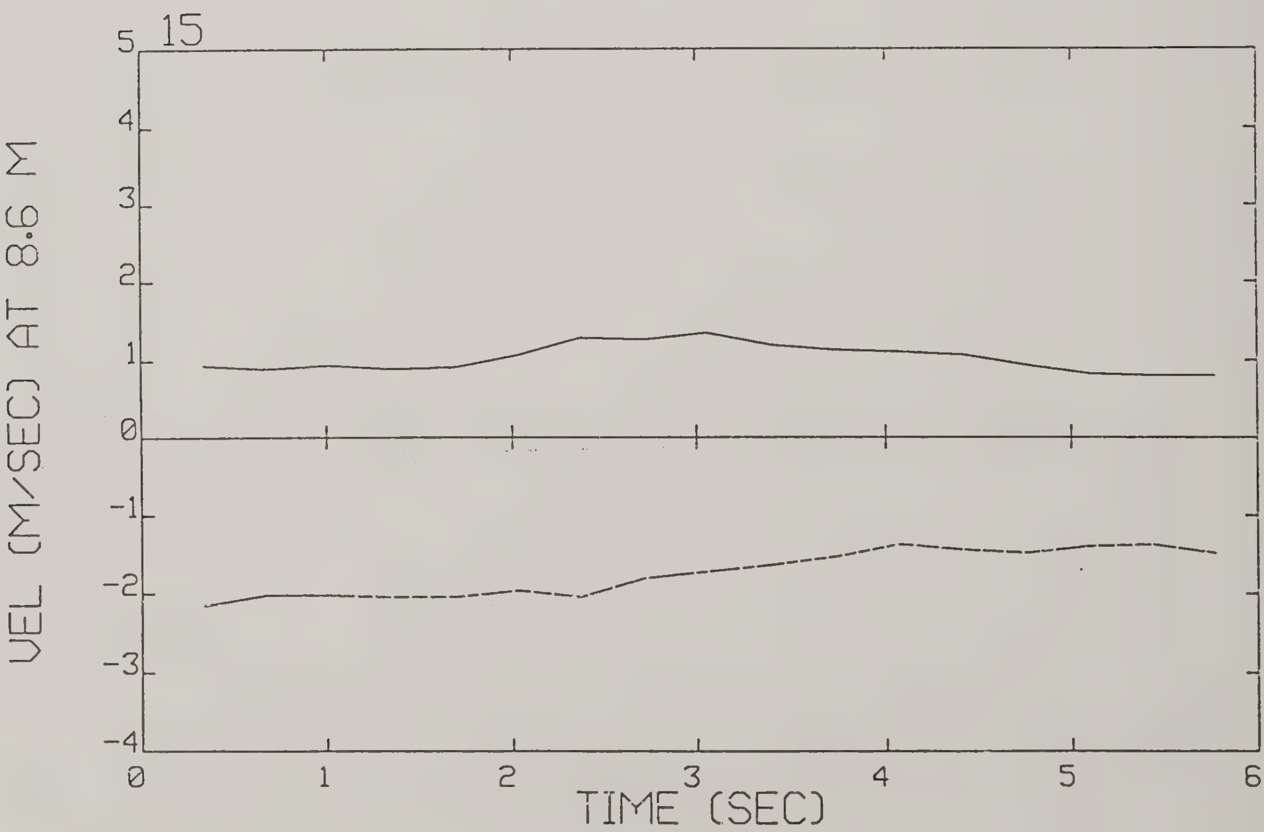

Figure 4-14: Velocities for run 15 at Dugway.

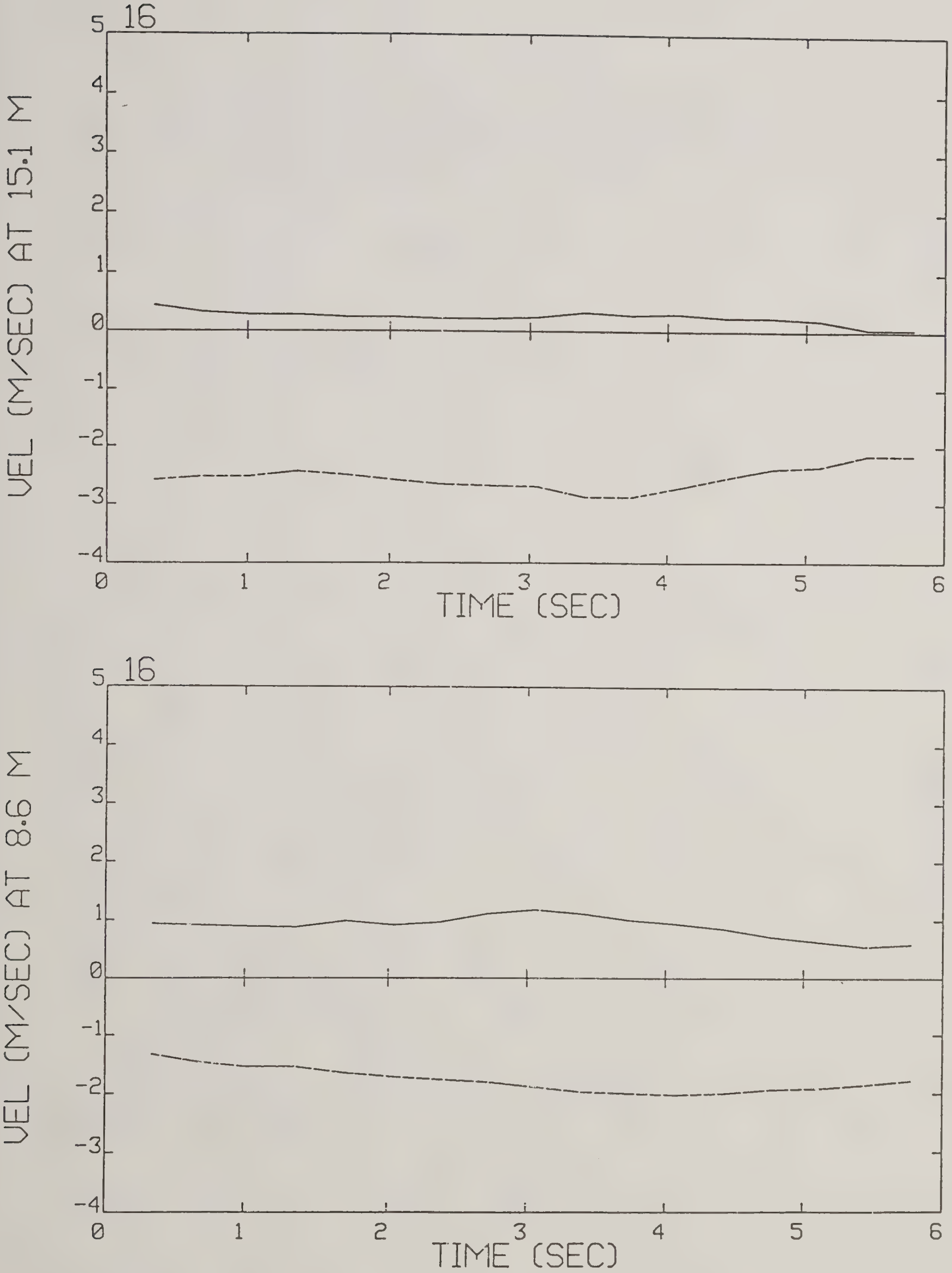

Figure 4-15: Velocities for run 16 at Dugway.

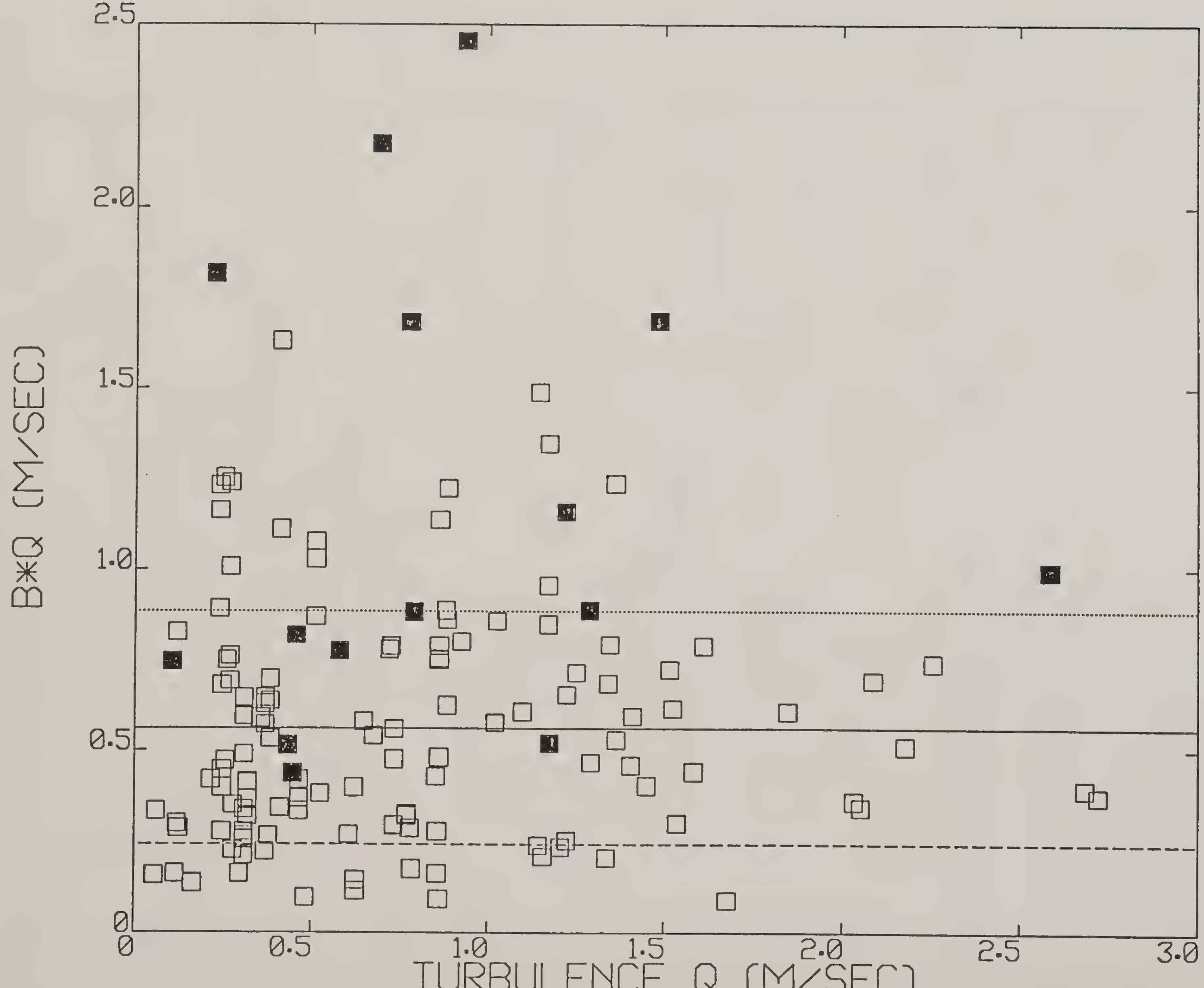

Figure 4-16: The behavior of the product bq with turbulence level q . Each square represents one of the applicable test runs: WIND (open squares); Dugway (filled squares). The solid line is the mean of the WIND data; the dashed lines represent the standard

5. CONCLUSIONS

Dugway high speed aircraft tower anemometer data has been shown to be consistent with the lower speed tower data from Program WIND. This suggests that a decay parameter of

$$bq = 0.56 \text{ m/sec} \tag{5-1}$$

could be used across all aircraft flight speeds in AGDISP and FSCBG.

6. REFERENCES

1. Teske, M.E.: "AGDISP Analysis of Vortex Decay from Program WIND Phases I and III," Continuum Dynamics, Inc. Technical Note 88-06, April 1988.

2. Teske, M.E.: "AGDISP User Manual Mod 5.0," Continuum Dynamics, Inc. Technical Note 88-09, June 1988.

3. Bjorklund, J.R, Bowman, C.R. and Dodd, G.C.: "User Guide - Forest Service Aerial Spray Computer Model FSCBG," USDA Forest Service, Forest Pest Management FPM 88-5.

4. Donaldson, C. duP. and Bilanin, A.J.: "Vortex Wakes of Conventional Aircraft," AGARDograph No. 204, May 1975.

United States
Department of
Agriculture

NATIONAL
AGRICULTURAL
LIBRARY

Advancing Access to
Global Information for
Agriculture